

Q-Tuning: Queue-based Prompt Tuning for Lifelong Few-shot Language Learning

Yanhui Guo^{1‡*} Shaoyuan Xu^{2‡} Jinmiao Fu^{2‡}
Jia Liu^{2,3} Chaosheng Dong² Bryan Wang²

¹McMaster University, Canada ²Amazon, USA ³The Ohio State University, USA
{guoy143}@mcmaster.ca {shaoyux, jinmiaof, hliujia, chaosd, brywan}@amazon.com

Abstract

This paper introduces **Q-tuning**, a novel approach for continual prompt tuning that enables the lifelong learning of a pre-trained language model. When learning a new task, Q-tuning trains a task-specific prompt by adding it to a prompt queue consisting of the prompts from older tasks. To better transfer the knowledge of old tasks, we design an adaptive knowledge aggregation technique that reweighs previous prompts in the queue with a learnable low-rank matrix. Once the prompt queue reaches its maximum capacity, we leverage a PCA-based eviction rule to reduce the queue’s size, allowing the newly trained prompt to be added while preserving the primary knowledge of old tasks. In order to mitigate the accumulation of information loss caused by the eviction, we additionally propose a globally shared prefix prompt and a memory retention regularization based on information theory. Extensive experiments demonstrate that our approach outperforms the state-of-the-art methods substantially on continual prompt tuning benchmarks. Moreover, our approach enables lifelong learning on linearly growing task sequences while requiring constant complexity for training and inference.

1 Introduction

In recent years, pretrained language models (LMs) have achieved huge success in natural language processing (Brown et al., 2020; Fu et al., 2022; Thoppilan et al., 2022; Jia et al., 2023; OpenAI, 2023), which popularizes the pretraining-finetuning pipeline in applications. However, with the ever-growing parameter scale of modern LMs (e.g., GPT-4 that may have 1.76 trillion parameters (OpenAI, 2023)), it becomes increasingly difficult to finetune the whole model, leading to extensive attention to parameter-efficient finetuning (PEFT) technologies. *Prompt tuning* (PT) (Liu et al., 2022)

has recently emerged as a leading PEFT solution. PT trains soft prompts and prepends them to the input of LMs, while keeping the LM parameters frozen. Existing works (Lester et al., 2021; Liu et al., 2023) have shown that PT can achieve performance on par with finetuning, while requiring fewer than 0.01% of the total trainable parameters. Continual prompt tuning (CPT) is a methodology that extends PT to the continual learning (CL) paradigm for learning new tasks that arrive in a *sequential* fashion.

CPT encounters technical challenges akin to those faced by traditional CL methods, including the well-known *catastrophic forgetting* (CF) (Lin et al., 2022) and *forward knowledge transfer* (FKT). To overcome these challenges, Wang et al. (2022b) designed a dual prompt tuning framework including a globally shared prompt and a task-specific prompt. However, continuously optimizing the shared prompt for new tasks will make the learned knowledge from old tasks vanish, leading to less efficient FKT. To improve the FKT, ProgPrompt was proposed by Razdaibiedina et al. (2023) which maintains a prompt list for incoming tasks by progressively adding newly trained prompts while storing all previously trained prompts. Following a similar strategy to extending the prompt list, Smith et al. (2023) proposed a prompt set expansion method by weighting the sum over a group of prompt components for each task. Although these methods succeed in improving the FKT, they suffer from the same problem when the length of prompts grows linearly at a rate of $\mathcal{O}(N)$ along with the number of tasks. This leads to an $\mathcal{O}(N^2)$ complexity for transformer-based models. Consequently, the training and inference costs will become intractable as N increases and exceeds a finite computation resource limit.

In this paper, we overcome the aforementioned challenges by proposing a novel continual prompt tuning technology named *Queue-based prompt tun-*

[‡] Equal contribution.

* Work done during internship at Amazon.

ing (**Q-tuning**). Q-tuning manages a *Queue-based prompt (Q-prompt)*, which is stored in a *finite-size* data buffer. For learning a new task, Q-tuning trains a new prompt combined with the fixed Q-prompt that stores all previously learned prompts. Upon the completion of tuning, the latest trained prompt will be added to the Q-prompt for the tuning of the next task. Once the number of tasks exceeds the queue-size limit, we will remove less informative prompts according to a principal component analysis (PCA) based dequeue rule. This endows Q-tuning with the ability to perform lifelong prompt tuning on extremely long task sequences. Our key contributions and results can be summarized as follows:

- We propose a continual prompt tuning method called Q-tuning that, to our knowledge, is the first technique to achieve lifelong learning in application scenarios with an agnostic number of new tasks through prompt tuning.
- Q-tuning consists of a prompt queue (Q-prompt) and an adaptive knowledge aggregation low-rank matrix that is optimized to capture the importance of the enqueued prompts to enhance FKT. A novel dequeue rule based on PCA is applied to trim the Q-prompt when it is full. In addition, a globally shared prefix prompt with a memory retention (MR) technique is devised to mitigate the information loss due to dequeuing.
- We conduct extensive experiments to demonstrate the successful applications of our proposed Q-tuning on few-shot CL tasks. Q-tuning outperforms all the competing CL methods by a large margin. In addition, Q-tuning highlights its ability to facilitate lifelong learning. For instance, our experiments on extremely long learning sequences consisting of 70 disjoint tasks have shown a 30% accuracy improvement over the standard prompt tuning method.

2 Related work

1) Continual Learning: Continual Learning (CL), also known as lifelong learning, is to learn from a stream of different tasks arriving sequentially. The major challenge of CL is to prevent the CF problem (Kemker et al., 2018) and achieve knowledge transfer (Ke et al., 2021). Existing CL approaches can be divided into three categories: 1) Memory-based methods (Shin et al., 2017; Bang et al., 2021; Jiao et al., 2022; Ermis et al., 2022) that store previous data and replay them when training on the next task

to mitigate CF issue; 2) Regularization-based methods (Kirkpatrick et al., 2017; Zenke et al., 2017; Schwarz et al., 2018) that apply an additional regularization loss to constrain the update of parameters that are less important to learning new tasks; 3) Architecture-based methods that dynamically expand the network capacity (Rusu et al., 2016; Yoon et al., 2018) or train new task-specific parameters (Yoon et al., 2020) while fixing parameters for old tasks to prevent forgetting. However, these methods require finetuning all model parameters and are too expensive to put into practice for large-scale models with an astronomical number of parameters, such as large language models (LLMs).

2) Prompt Tuning: Prompt tuning (Lester et al., 2021; Li and Liang, 2021; Gu et al., 2022; Jia et al., 2022; Wang et al., 2023) is a lightweight approach to finetune an LLM model for a target task, which only requires optimizing a series of virtual tokens (a.k.a “soft prompt”) instead of updating the entire model. It has been demonstrated that prompt tuning can achieve the same or even better performance than training a full model. In prompt tuning, a trainable soft prompt $\theta_{\mathcal{P}}$ is prepended to the input text \mathbf{x} while keeping other parameters frozen. In this case, the combined model parameters include trainable prompt parameters $\theta_{\mathcal{P}}$ and parameters $\theta_{\mathcal{M}}$ of a pretrained model \mathcal{M} . Given the task $\mathcal{T} = (\mathcal{X}, \mathcal{Y})$ consisting of training pairs (\mathbf{x}, \mathbf{y}) , the objective of prompt tuning is:

$$\max_{\theta_{\mathcal{P}}} \sum_{(\mathbf{x}, \mathbf{y}) \in \mathcal{T}} \log p(\mathbf{y} | \mathbf{x}; \theta_{\mathcal{M}}, \theta_{\mathcal{P}}). \quad (1)$$

3) Continual Prompt Tuning: Many works (Zhu et al., 2022; Yin et al., 2022; Ermis et al., 2022; Wang et al., 2022b; Razdaibiedina et al., 2023) have applied prompt tuning to the continual learning domain, but we observe some limitations of these methods. For example, the techniques proposed by Zhu et al. (2022); Ermis et al. (2022) require a large data buffer to store training samples from previous tasks for anti-forgetting. The paradigms of progressively extending the prompts (Razdaibiedina et al., 2023; Wang et al., 2022a; Smith et al., 2023) are inapplicable to the scenario with an infinitely increasing number of tasks.

To address the aforementioned limitations, we introduce Q-tuning, which is data-buffer-free and enables anti-forgetting lifelong learning in the face of an ever-expanding stream of tasks.

3 The Q-Tuning Approach

3.1 Q-prompt and Update Rule

Q-prompt: Given the continually increased task set $\mathcal{T} = \{(\mathcal{X}^1, \mathcal{Y}^1), (\mathcal{X}^2, \mathcal{Y}^2), \dots, (\mathcal{X}^i, \mathcal{Y}^i)\}$, where $\mathcal{T}^i = (\mathcal{X}^i, \mathcal{Y}^i)$ denotes the training pairs on i -th task, a naive solution is maintaining an increased prompt list (Razdaibiedina et al., 2023) $[\theta_{\mathcal{P}}^1, \theta_{\mathcal{P}}^2, \dots, \theta_{\mathcal{P}}^i]$, where $[\cdot, \cdot]$ is the concatenation operation. The objective for the i -th task is:

$$\max_{\theta_{\mathcal{P}}^i} \sum_{(\mathbf{x}^i, \mathbf{y}^i) \in \mathcal{T}^i} \log p(\mathbf{y}^i | \mathbf{x}^i; \theta_{\mathcal{M}}, \underbrace{[\theta_{\mathcal{P}}^1, \theta_{\mathcal{P}}^2, \dots, \theta_{\mathcal{P}}^i]}_{\text{prompt list for } N \text{ tasks}}). \quad (2)$$

For each task, only the newly appended prompt is trainable, while the previously trained prompts are fixed. However, when N grows asymptotically (*i.e.*, the model is set as a lifelong learner), training the extremely long prompt list becomes intractable due to the finite system resources. This motivates us to propose the Q-tuning technique.

Fig. 1 illustrates the overall framework of the Q-tuning technique. In Q-tuning, we add a new trainable prompt to a prompt queue \mathcal{Q} that stores all previously trained prompts for old tasks. This updated \mathcal{Q} associated with a globally shared prefix prompt will be tuned for the new task while keeping the prior prompts in \mathcal{Q} frozen. This progressively appending approach enables forward knowledge transfer as the old task’s information is saved in the Q-prompt. We let $C = l \times \mathcal{Q}_{\text{size}}$ denote the maximum capacity of the Q-prompt \mathcal{Q} , where l is the length of a single prompt per task and $\mathcal{Q}_{\text{size}}$ is the maximum number of prompts in the queue. When reaching the capacity limit of \mathcal{Q} , the Q-prompt will be trimmed using an eviction rule to remove less informative prompts and append new trainable prompts for future tasks.

Knowledge Aggregation for FKT: In Q-tuning, all prompts in the memory (*i.e.*, the Q-prompt \mathcal{Q}), as well as the pretrained LM model, are frozen when learning a new task. Consequently, the LM model will be forced to take these fixed prompts in the queue as inputs without considering their relevance to the current task, leading to suboptimal performance. To address this problem, we propose a prompt-based knowledge aggregation mechanism. For task i , we use a trainable matrix $\mathcal{W}^i \in \mathbb{R}^{c^i \times d}$, which is of the same dimension as the Q-prompt \mathcal{Q}^i , to scale \mathcal{Q}^i by $\mathcal{W}^i \circ \mathcal{Q}^i$ (\circ denotes the Hadamard product). Here, for task i , we

denote the total prompt length of \mathcal{Q}^i by $c^i = l \times i$. Since directly optimizing a large-scale matrix of size $c^i \times d$ is costly, we propose a low-rank multiplicative method inspired by Aghajanyan et al. (2021). The weight matrix \mathcal{W}^i can be expressed as $\mathcal{W}^i = \mathbf{u}_i \otimes \mathbf{v}_i^T$, where $\mathbf{u}_i \in \mathbb{R}^{c^i}$, $\mathbf{v}_i \in \mathbb{R}^d$ and \otimes denotes the outer product. Clearly, \mathcal{W}^i is a rank-one matrix, and the number of trainable parameters is reduced to $c^i + d \ll c^i \times d$. We jointly optimize the newly appended prompt $\theta_{\mathcal{P}}^i$ and the low-rank aggregation matrix \mathcal{W}^i by maximizing the cross-entropy loss as follows:

$$\max_{\theta_{\mathcal{P}}^i, \mathcal{W}^i} \sum_{(\mathbf{x}^i, \mathbf{y}^i) \in \mathcal{T}^i} \log p(\mathbf{y}^i | \mathbf{x}^i; \theta_{\mathcal{M}}, \mathcal{W}^i \circ \underbrace{\mathcal{Q}^i(\theta_{\mathcal{P}}^1, \dots, \theta_{\mathcal{P}}^i)}_{\text{maximum length is } C=l \times \mathcal{Q}_{\text{size}}}), \quad (3)$$

where only the new added prompt $\theta_{\mathcal{P}}^i$ and the weight matrix \mathcal{W}^i for the i -th task are trainable.

De-Q Rule: Our Q-prompt design allows appending newly trained prompts until they reach the maximum length. Once the Q-prompt is full (denoted by \mathcal{Q}_C), a dequeuing (De-Q) rule is executed to reduce the length of \mathcal{Q}_C to $C - l$ to add the new prompt. However, this leads to a challenge: *how to retain the most useful prompt information after trimming the Q-prompt?* Straightforward De-Q rules include random eviction and first in first out (FIFO). However, these simple rules may discard valuable information in the queue, resulting in negative impacts on FKT.

To address the above problem, we introduce a simple yet effective De-Q rule named DQ-PCA based on principal component analysis (PCA) (Shlens, 2014). Specifically, we first calculate the centered Q-prompt $\tilde{\mathcal{Q}}_C \in \mathbb{R}^{C \times d}$ with a zero mean: $\tilde{\mathcal{Q}}_C = \mathcal{Q}_C - \text{mean}(\mathcal{Q}_C)$. Then we perform singular value decomposition (SVD). We extract the first $C - l$ principal components to obtain the trimmed Q-prompt $\tilde{\mathcal{Q}}_{C-l} \in \mathbb{R}^{(C-l) \times d}$ and enqueue the new trainable $\theta_{\mathcal{P}}^i \in \mathbb{R}^{l \times d}$. This process can be written as follows:

$$\text{SVD}(\tilde{\mathcal{Q}}_C) = U \Sigma V^T, \tilde{\mathcal{Q}}_{C-l} = \Sigma_{C-l} V_{C-l}^T, \quad (4)$$

$$\mathcal{Q}_C \xleftarrow{\text{Update}} \tilde{\mathcal{Q}}_{C-l} \oplus \theta_{\mathcal{P}}^i, \quad (5)$$

where \oplus denotes the concatenation operation $[\tilde{\mathcal{Q}}_{C-l}, \theta_{\mathcal{P}}^i]$, $U \in \mathbb{R}^{C \times C}$ is the matrix consisting of the left singular vectors, $\Sigma \in \mathbb{R}^{C \times d}$ is the diagonal matrix formed by the singular values in decreasing

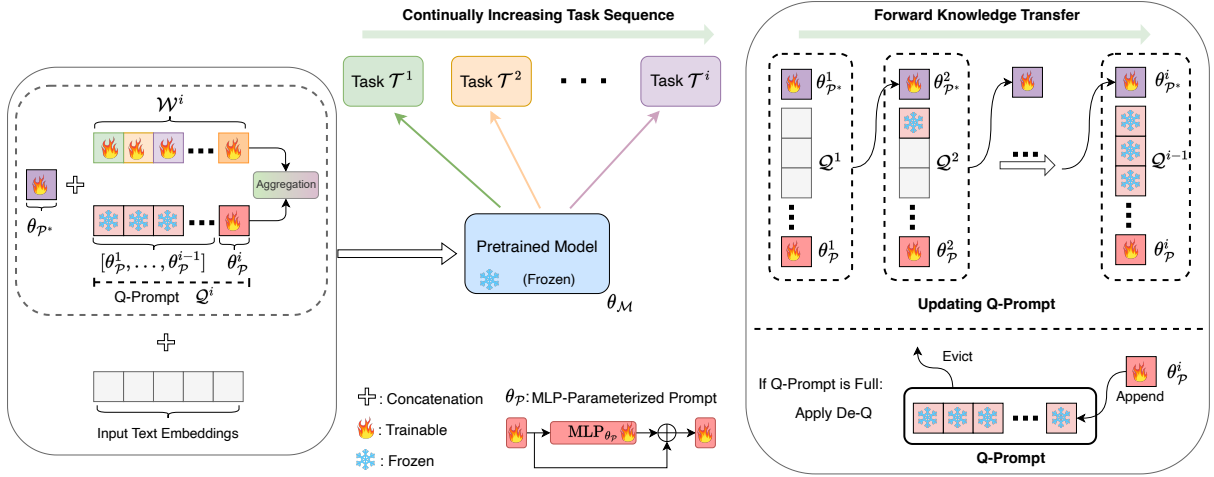


Figure 1: The overall framework of the proposed **Q-tuning** technology. Given a continually growing-up task sequence, we propose a prompt queue (Q-prompt) and a globally *shared* prefix prompt $\theta_{P^*}^i$ to achieve the forward knowledge transfer, where the superscript of $\theta_{P^*}^i$ denotes the i -th status. Moreover, we adopt a knowledge aggregation method to adaptively adjust the contribution of each fixed prompt $[\theta_{P^*}^1, \theta_{P^*}^2, \dots, \theta_{P^*}^{i-1}]$ in Q-prompt by using a rank-one matrix \mathcal{W}^i . We parameterize the trainable soft prompt by a two-layer residual MLP. If the length of the Q-prompt exceeds the limit, we apply a De-Q rule to discard less informative prompts in the queue.

order and V^T is the matrix of right singular vectors. The matrix V_{C-l}^T is formed by the top $C-l$ principle row vectors of V^T and $\Sigma_{C-l} \in \mathbb{R}^{(C-l) \times (C-l)}$ denotes the diagonal matrix with the top $C-l$ singular values. When the length of the Q-prompt exceeds C , it will trigger the DQ-PCA to shrink the Q-prompt's length to $C-l$. As a result, Q-tuning achieves an $\mathcal{O}(1)$ training and inference complexity instead of $\mathcal{O}(N^2)$ for transformer-based LMs, thereby enabling low-cost lifelong learning¹.

3.2 Prefix Prompt for Knowledge Sharing

Although DQ-PCA is able to minimize information loss by keeping the most useful information from previous prompts in the queue, information loss will inevitably accumulate as the number of tasks grows larger. To avoid such loss, we introduce a globally shared prefix prompt, θ_{P^*} . This prefix prompt is appended to the head of the Q-prompt and continually trained across all the tasks for aggregating the global information. However, continuously training the shared prompt θ_{P^*} will make it lean toward the newest task. To address this limitation, we propose a *memory retention* (MR) regularization by maximizing the overlapping information between the shared prefix prompt and the learned knowledge from old tasks. For each

task i , we formulate the maximization problem as:

$$\max_{\theta_{P^*}^i} I(\underbrace{p(\mathbf{y}^i | \mathbf{x}^i; \theta_M, \theta_{P^*}^i)}_{p(\xi^i)}; \underbrace{p(\mathbf{y}^i | \mathbf{x}^i; \theta_M, \mathcal{W}^{i-1} \circ [\theta_{P^*}^{i-1}, Q^{i-1}])}_{p(\xi^{i-1})}), \quad (6)$$

where $I(\cdot, \cdot)$ represents the mutual information between two random variables, $\theta_{P^*}^i$ denotes the shared prompt to be learnt for i -th task, $\theta_{P^*}^{i-1}$ is the shared prompt learnt until task $i-1$, and Q^{i-1} denotes the Q-prompt until task $i-1$. The second term $p(\xi^{i-1})$ in Eq. (6) represents the old knowledge learnt before the i -th task, provided by the shared $\theta_{P^*}^{i-1}$ and the Q-prompt Q^{i-1} . Maximizing Eq. (6) can transfer the old knowledge modeled by $p(\xi^{i-1})$ to current shared prompt $\theta_{P^*}^i$. Such regularization can mitigate the information loss caused by trimming Q^{i-1} when the Q-prompt Q^{i-1} at task $i-1$ reaches its maximum length. As a result, the full information prior to the new task $i+1$ can be represented by the union of Q^i and $\theta_{P^*}^i$.

To solve the mutual information $I(p(\xi^i); p(\xi^{i-1}))$ in Eq. (6), we adopt the mutual information estimator² (Hjelm et al., 2018; Poole et al., 2019) based on the Jensen-Shannon divergence (JSD), which satisfies:

$$\begin{aligned} I(p(\xi^i); p(\xi^{i-1})) &:= \mathcal{D}_{\text{JSD}}(\mathbf{J}; \mathbf{M}) \\ &\geq \mathbb{E}_{z \sim \mathbf{J}} [-\sigma(-\mathcal{F}_\omega(z))] - \mathbb{E}_{z' \sim \mathbf{M}} [\sigma(\mathcal{F}_\omega(z'))], \end{aligned} \quad (7)$$

¹For example, on a single NVIDIA V100 GPU (32GB) with the same training setting as ProgPrompt (Razdaibiedina et al., 2023), Q-tuning can easily handle an extremely long 70-task sequence, while ProgPrompt fails due to memory overflow (cf. our experiments).

²More details about the deviation of the mutual information estimator can be found in Appendix B.

where $\mathbf{J} = p(\xi^i, \xi^{i-1})$ and $\mathbf{M} = p(\xi^i)p(\xi^{i-1})$ are the joint and the product of marginals of the random variables ξ^i and ξ^{i-1} , respectively, and $\sigma(t) = \log(1 + e^t)$. \mathcal{F}_ω is a discriminator function (Nowozin et al., 2016) modeled by an auxiliary neural network with parameters ω .

3.3 Objective Function of Q-Tuning

Given the i -th classification task, the training objective of Q-tuning is defined as:

$$\mathcal{L}_{\mathcal{Q}}(\theta_{\mathcal{P}^*}^i, \theta_{\mathcal{P}}^i, \mathcal{W}^i) = - \sum_{(\mathbf{x}^i, \mathbf{y}^i) \in \mathcal{T}^i} \log p(\mathbf{y}^i | \mathbf{x}^i; \theta_{\mathcal{M}}, \theta_{\mathcal{P}^*}^i, \mathcal{W}^i \circ \mathcal{Q}^i(\theta_{\mathcal{P}}^1, \dots, \theta_{\mathcal{P}}^i)), \quad (8)$$

where \mathcal{T}^i denotes the data streams of the i -th task. The pretrained model $\theta_{\mathcal{M}}$ and all the enqueued prompts prior to i -th task are fixed. The trainable parameters include the shared prefix prompt $\theta_{\mathcal{P}^*}^i$, the newly appended prompt $\theta_{\mathcal{P}}^i$ and the queue aggregation matrix \mathcal{W}^i .

For the prefix prompt $\theta_{\mathcal{P}^*}^i$, we enable its capability for memorizing the knowledge of old tasks with the MR regularization defined by Eq. (6). According to Eq. (7), we can maximize the lower bound of the mutual information, which can be rewritten as minimizing a loss \mathcal{L}_{MR} with respect to $\theta_{\mathcal{P}^*}^i$:

$$\mathcal{L}_{\text{MR}}(\theta_{\mathcal{P}^*}^i) = -\mathbb{E}_{z \sim \mathbf{J}} [-\sigma(-\mathcal{F}_\omega(z))] + \mathbb{E}_{z' \sim \mathbf{M}} [\sigma(\mathcal{F}_\omega(z'))], \quad (9)$$

where \mathbf{J} and \mathbf{M} are defined in Eq. (6) and Eq. (7). The MLP-based discriminator $\mathcal{F}_\omega(\cdot)$ consists of two 512-unit hidden layers. To optimize Eq. (9) on a given finite training data set, we approximate the expectations using minibatch samples as in Belgazi et al. (2018).

Putting all things together, we obtain the overall loss:

$$\mathcal{L}_{\text{total}} = \mathcal{L}_{\mathcal{Q}}(\theta_{\mathcal{P}^*}^i, \theta_{\mathcal{P}}^i, \mathcal{W}^i) + \eta \mathcal{L}_{\text{MR}}(\theta_{\mathcal{P}^*}^i), \quad (10)$$

where η is called ‘‘memory factor’’ which is used to weigh the contribution of \mathcal{L}_{MR} . When the number of tasks $N \leq C$, we set $\eta = 0$, whereas if $N > C$, we set $\eta > 0$. We empirically find the best η as reported in Table 12 of Appendix D. Algorithm 1 summarizes the Q-tuning algorithm.

4 Experiment Settings

4.1 Datasets and Baseline Methods

Datasets: Following Razdaibiedina et al. (2023), we evaluate the proposed Q-tuning using two

few-shot CL benchmark settings including short-sequence experiments, long-sequence experiments, and lifelong learning experiments.

In the short-sequence CL experiments, we adopt five text classification datasets (Zhang et al., 2015), including YP reviews, Amazon reviews, DBpedia, Yahoo Answers, and AG News. To validate our method’s efficacy on different model backbones, we adopt the T5-large model and the BERT-base model for evaluation. For the T5 experiments, we use three different orders (*i.e.*, Orders 1~3³) composed of the AG News, Amazon, Yahoo, and DBpedia datasets by following the few-shot CL setting as in Qin and Joty (2021); Razdaibiedina et al. (2023). For the BERT experiments, we use four different orders (*i.e.*, Orders 4~7³) including all the above five tasks, and we use the same train and test split as IDBR (Huang et al., 2021) including 115,000 training and 7,600 test examples.

In the long-sequence CL experiments, following Razdaibiedina et al. (2023), we choose 15 different tasks, which consist of the aforementioned five datasets from the short-sequence CL benchmark, four tasks from GLUE benchmark (MNLI, QQP, RTE, SST2) by Wang et al. (2018), five tasks from SuperGLUE benchmark by Wang et al. (2019) (WiC, CB, COPA, MultiRC, BoolQ), and IMDB movie reviews dataset (Maas et al., 2011). We use three different orders (*i.e.*, Orders 8~10³).

Lastly, to mimic the lifelong learning scenario, we further add the Banking77 dataset (Casanueva et al., 2020), the Emotion dataset (Saravia et al., 2018), the rest datasets (WNLI, COLA and QNLI) of the GLUE benchmark, and WSC of the SuperGLUE benchmark. We construct a benchmark with a long sequence of 70 tasks by splitting the datasets with over 4 classes into *disjoint* subsets⁴. Following Razdaibiedina et al. (2023), for each task, we randomly select 500 samples per class from the training set for validation, and use early stopping based on the validation accuracy.

Baseline Methods for Comparison: In the experiments, we compare our model with 11 baseline methods including: (1) **Per-task Finetune** (Razdaibiedina et al., 2023), (2) **Continual Finetune** (Wang et al., 2020; Huang et al., 2021), (3) **Prompt**

³The details of each order are reported in Table 9 of the Appendix. For each order, as in Razdaibiedina et al. (2023), we train three versions of models, with 16 (or 20), 200, and 1000 training samples per class respectively, and report the performance on the test sets correspondingly.

⁴Please refer to Appendix C.1 and Appendix C.2.

Tuning (Qin and Joty, 2021; Lester et al., 2021), (4) **Data Replay** (Autume et al., 2019), (5) **EWC** (Kirkpatrick et al., 2017), (6) **A-GEM** (Chaudhry et al., 2018), (7) **LFPT5** (Qin and Joty, 2021), (8) **MBPA++** (Autume et al., 2019), (9) **IDBR** (Huang et al., 2021), (10) **Per-task Prompt** (Lester et al., 2021), and (11) **ProgPrompt** (Razdaibiedina et al., 2023)⁵.

Method	DR	Order			avg
		1	2	3	
Per-task Finetune [‡]		70.0	70.0	70.0	70.0
Continual Finetune [□]		18.9	24.9	41.7	28.5
Data Replay	✓	35.4	37.1	41.5	38.0
EWC [□]		39.0	38.0	44.8	40.6
LFPT5 ^{*□}	✓	47.6	52.6	57.9	52.7
ProgPrompt [*]		74.1	74.2	75.3	74.5
Ours [*]		75.8	75.8	76.9	76.2

(a) Results with the T5-large model.

Method	DR	Order				avg
		4	5	6	7	
Per-task Finetune [‡]		73.9	73.9	73.9	73.9	73.9
Continual Finetune [◇]		14.8	27.8	26.7	4.5	18.4
Data Replay [◇]	✓	67.2	64.7	64.7	44.6	57.8
A-GEM [◇]	✓	70.6	65.9	67.5	63.6	66.9
MBPA++ [◇]	✓	70.8	70.9	70.2	70.7	70.6
IDBR [†]	✓	75.9	76.2	76.4	76.7	76.3
ProgPrompt [*]		77.8	77.5	77.6	77.4	77.6
Ours [*]		78.5	78.3	78.3	78.4	78.4

(b) Results with the BERT-base model.

Table 1: Summary of the results with T5 and BERT models on the short-sequence benchmark⁶. Average accuracy after training on the last task is reported. All results are averaged over 3 runs. For the T5 model, we follow few-shot CL settings as in Qin and Joty (2021).

4.2 Implementation Details

Q-tuning is a model-backbone-agnostic approach that is applicable to any language model, such as the GPT series (OpenAI, 2023), regardless of their sizes. Due to resource constraints, following Razdaibiedina et al. (2023), we use two popular language models including the encoder-decoder T5 model (Raffel et al., 2020) and encoder-only BERT model (Devlin et al., 2018) in our experiments. For all the T5 experiments, we adopt the T5-large model with the text-to-text formulation, where classification labels are mapped into words (e.g. 0/1 will be mapped as “True”/“False”). For all the BERT experiments, we use the BERT-base

⁵More introductions to these competing methods are provided in Appendix C.3 due to space limitation.

⁶Methods marked with * use soft prompt, while other methods train the entire model. For ProgPrompt, the results are reported by running their released code. DR denotes whether the data replay is required. □, ◇, † and ‡ mark the results from Qin and Joty (2021), Autume et al. (2019), Huang et al. (2021), and Razdaibiedina et al. (2023), respectively.

model as in IDBR and MBPA++ methods (Huang et al., 2021; Autume et al., 2019). We use the representation of the first token $h_{[CLS]}$ to predict the class of the input text, where $h_{[CLS]}$ is encoded by a beginning-of-a-sentence symbol [CLS]. Following Razdaibiedina et al. (2023), we apply a linear head including a linear transformation parameterized by α and a softmax function to obtain the classification probabilities over classes $k \in \{1 \dots \mathcal{K}\}$: $p(y = k|h) = \frac{\exp(\alpha_k h_{[CLS]})}{\sum_{y \in \mathcal{K}} \exp(\alpha_y h_{[CLS]})}$. The linear head is trained separately for each task. In our experiments, the prompt length per task is set to 10, and each prompt is parameterized by a two-layer MLP⁷.

5 Experimental Results

We report Q-tuning performance on T5-large and BERT-base models and compare it to previous CL and prompt tuning approaches. We evaluate the methods after training on all tasks and report the averaged test set accuracy across all tasks. The detailed experimental metrics are reported in Appendix C.1. All the experiments are conducted on a single 32GB NVIDIA V100 GPU.

5.1 Results on Few-shot CL Benchmarks

Short-sequence Experiments: Following ProgPrompt (Razdaibiedina et al., 2023), we evaluate the performance of Q-tuning on the standard short-sequence CL benchmarks with few-shot learning settings, where Orders 1~3 and Orders 4~7 are evaluated with the T5 and BERT models, respectively. Since these sequential tasks only consist of four or five disjoint datasets, we set $Q_{\text{size}} = 5$ for the Q-prompt without utilizing the DQ-PCA rule. In Table 1a, we compare Q-tuning with the existing CL, prompt tuning, and continual prompt tuning approaches using the T5 model. Q-tuning outperforms all the CL approaches by a large margin, achieving 76.2% accuracy on average of all the orders. Q-tuning increases the accuracy by 1.7% (from 74.5% to 76.2%) compared to ProgPrompt, the SOTA approach of continual prompt tuning. Q-tuning also surpasses the “Per-task Finetune” by 6.2% on average, demonstrating the efficacy of the proposed queue aggregation and shared prefix prompt approach in enhancing the FKT capability. Table 1b reports the results on the BERT-base model that verify a consistent improvement.

⁷The experimental details are reported in Appendix C.3.

Method	T5-large				BERT-base				
	Order 8	Order 9	Order 10	Average	Order 8	Order 9	Order 10	Average	
Continual Finetune	9.3	9.5	10.4	9.7	29.9	30.5	33.6	31.3	
Prompt Tuning*	9.7	24.4	12.2	17.4	-	-	-	-	
Data Replay	46.0	50.3	34.6	43.6	34.9	39.3	34.9	36.4	
LFPT5*	54.7	54.1	54.2	54.3	-	-	-	-	
Per-task Prompt*	69.9	69.9	69.9	69.8	50.6	50.6	50.6	50.6	
IDBR	-	-	-	-	39.7	37.9	32.9	36.8	
ProgPrompt*	75.4	76.6	76.7	76.2	55.3	53.3	51.9	53.5	
Ours* ($Q_{size} = 5$)	Random	76.4	77.3	76.1	76.6	53.6	53.2	51.1	52.6
	FIFO	76.5	77.2	76.7	76.8	54.5	53.8	51.8	53.4
	DQ-PCA	77.5	78.8	77.8	78.0	55.6	56.0	51.8	54.5
Ours* ($Q_{size} = 10$)	Random	76.7	77.2	76.5	76.8	54.7	54.2	52.8	53.9
	FIFO	77.0	77.1	76.7	76.9	54.6	54.2	52.9	53.9
	DQ-PCA	78.3	79.7	78.7	78.9	56.5	56.2	52.6	55.1
ProgPrompt + Aggregation + θ_{P^*} MTL		79.0	79.1	78.1	78.7	55.3	55.2	54.5	55.0
		70.7	70.7	70.7	70.7	56.9	56.9	56.9	56.9

Table 2: Average test set performance of Q-tuning and prior approaches on long-sequence experiments with 15 text classification tasks in different orders. In the experiments⁸, we use the few-shot CL by setting 20 samples per class. All the results are averaged over 3 runs.

Long-sequence Experiments: In Table 2, we compare the Q-tuning with the baseline approaches on the long-sequence CL benchmark, including Orders 8~10 using the T5-large and the BERT-base models. These experiments consist of 15 tasks in three different orders. We follow the few-shot CL setting as in Razdaibiedina et al. (2023) by selecting 20 samples per class. The row of “ProgPrompt + θ_{P^*} ” denotes the results by adding the shared prompt to ProgPrompt, while maintaining its complete prompt list of 15 prompts. We can observe that setting the maximum length of the Q-prompt to 5 using DQ-PCA only leads to a 0.7% accuracy drop (from 78.7% to 78.0%) compared with the “ProgPrompt + Aggregation + θ_{P^*} ”. Moreover, we even observe a 0.2% accuracy increase over the full prompt when setting the maximum Q-prompt length to 10. This indicates the capability of DQ-PCA to protect essential knowledge when trimming the Q-prompt.

In addition, in Table 2, we compare the proposed DQ-PCA with the two naive queue eviction rules including random dropping, first in and first out (FIFO). As the results suggest, evicting Q-prompt by random dropping and FIFO yields very close performance, which both blindly shrink the Q-prompt without considering the relevance across different prompts. Unlike them, our DQ-PCA shrinks the Q-prompt by preserving the most informative prompts, thus clearly outperforming those

⁸MTL denotes multi-task learning that finetunes the model using all the datasets from different tasks. Methods marked with * only train a soft prompt while freezing the pretrained model, other methods train the entire model. The “Full Prompts” denotes remaining all prompts in queue by setting $Q_{size} = 15$.

two naive strategies. The results on the T5-large and the BERT-base models collectively witness the superiority of using our DQ-PCA.

Method	T5-large			
	Order 11	Order 12	Order 13	Average
ProgPrompt ⁹	Fail	Fail	Fail	-
Per-task Prompt	60.4	60.4	60.4	60.4
Shared Prompt	62.4	62.7	63.1	62.7
Q-tuning ($Q_{size} = 10$)	90.9	90.6	90.8	90.8

Table 3: Results on extremely long sequence experiments (70 tasks). All results are averaged over 3 runs.

Lifelong Learning Experiments: Lastly, we use extremely long task sequences to mimic lifelong learning scenarios. Table 3 reports the results of Q-tuning on Orders 11~13 including three *random* permutations of 70 *disjoint* tasks. Training ProgPrompt will fail due to out of memory caused by the accumulation of prompts⁹. Compared to the per-task prompt tuning, Q-tuning has gained considerable performance benefits (30.4% accuracy improvement on average from 60.4% to 90.8%). This can be attributed to 1) the improved FKT by applying Q-prompt knowledge aggregation, 2) the effective trimming of Q-prompt using DQ-PCA to enable the training of long sequence of tasks, and 3) the use of MR regularization and shared prefix prompt to avoid the accumulated information loss caused by the Q-prompt trimming. We also compare Q-tuning with training using a global shared prompt and a per-task prompt plus the MR regularization for each task without maintaining

⁹When using the same batch size as Q-tuning, ProgPrompt encounters failure during training after the 15-th task.

a queue. To ensure a fair comparison, we set the length of the shared prompt to be identical to Q-tuning, *i.e.*, $l \times Q_{\text{size}}$. Although the accuracy of the shared prompt is better than the per-task prompt tuning (2.3% improvement on average from 60.4% to 62.7%), it is outperformed by Q-tuning by 28.1% (62.7% to 90.8%) on average. This indicates that, although the Q-prompt and the shared prefix prompt serve the same purpose of aggregating knowledge for better FKT, it is beneficial to keep both components.

Forward Transfer (Target Task)	Q-prompt (Full)	Q-prompt ($Q_{\text{size}} = 5$)	Q-prompt ($Q_{\text{size}} = 10$)	Prompt Tuning
Task 11	98.1	97.8 ($\downarrow 0.3\%$)	98.2 ($\uparrow 0.1\%$)	97.1 ($\downarrow 1.0\%$)
Task 12	86.2	83.9 ($\downarrow 2.3\%$)	86.1 ($\downarrow 0.1\%$)	72.6 ($\downarrow 13.6\%$)
Task 13	56.6	54.9 ($\downarrow 1.7\%$)	56.2 ($\downarrow 0.4\%$)	49.8 ($\downarrow 6.8\%$)
Task 14	50.4	50.3 ($\downarrow 0.1\%$)	50.5 ($\uparrow 0.1\%$)	47.6 ($\downarrow 2.8\%$)
Task 15	69.4	68.9 ($\downarrow 0.5\%$)	69.1 ($\downarrow 0.3\%$)	68.1 ($\downarrow 1.3\%$)
Average	72.1	71.2 ($\downarrow 0.9\%$)	72.0 ($\downarrow 0.1\%$)	67.0 ($\downarrow 5.1\%$)

Table 4: Forward knowledge transfer results of Order 9 using 20 samples/class. Results are averaged over 3 runs.

Sequence	Method			Num. samples			
	Q-prompt	Aggregation	θ_{P^*}	16	200	1000	Average
Short	✓	✗	✗	74.5	79.8	79.8	78.0
	✓	✓	✗	75.2	80.9	80.4	78.8
	✓	✗	✓	75.1	80.6	80.9	78.9
	✓	✓	✓	76.2	81.2	81.9	79.7
Sequence	Method			Num. samples			
	Q-prompt	Aggregation	θ_{P^*}	20	200	1000	Average
Long	✓	✗	✗	76.7	80.8	80.8	79.4
	✓	✓	✗	77.2	81.1	82.1	80.2
	✓	✗	✓	77.4	81.1	82.3	80.3
	✓	✓	✓	78.9	81.9	83.3	81.4

Table 5: Ablation studies on the Q-prompt aggregation and shared prefix prompt¹⁰. Results are averaged over 3 runs.

5.2 Ablation Study and Analysis

In this section, we evaluate our approach’s performances in various aspects, including its capability of fulfilling FKT, adapting previous prompts based on their relevance to the new task using the Q-prompt aggregation, and maintaining global knowledge sharing using a shared prefix prompt.

Forward Knowledge Transfer: In Table 4, we evaluate the FKT performance of the trimmed Q-prompt. We train three different Q-prompts including the “Full”, “ $Q_{\text{size}} = 5$ ” and “ $Q_{\text{size}} = 10$ ”, where the “Full” denotes keeping the complete Q-prompt without the De-Q operation. All these Q-prompts are continuously trained on the first 10 tasks of Order 9. Then we separately evaluate the FKT performance of these Q-prompts on five remaining target tasks. As a reference, we also train a single prompt (denoted by “Prompt Tuning” whose

¹⁰For long sequence, we set $Q_{\text{size}} = 10$. More detailed results of each order are reported in Appendix D.

token length is set the same as the total length of the full Q-prompt) on each target task. First of all, full Q-prompt substantially outperforms “Prompt Tuning”, demonstrating our approach’s capability in fulfilling FKT whereas “Prompt Tuning” does not leverage any information from other tasks. Moreover, compared to the full Q-prompt, the trimmed Q-prompt only has a minor performance drop. For example, setting $Q_{\text{size}} = 10$ only leads to 0.1% accuracy decrease (from 72.1% to 72.0%). This proves that trimmed Q-prompt is able to maintain FKT at the same level as the full Q-prompt, despite previous prompts being trimmed.

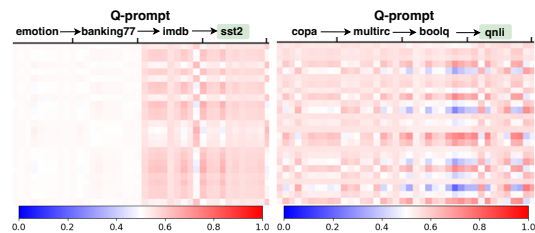


Figure 2: Visualization of aggregation matrix.

θ_{P^*}	Method		T5-large			
	Aggregation	\mathcal{L}_{MR}	Order 11	Order 12	Order 13	Average
✗	✗	✗	86.8	87.3	87.7	87.3
✓	✗	✗	87.6	88.1	88.7	88.1
✓	✓	✗	89.8	89.4	90.1	89.8
✓	✓	✓	90.9	90.6	90.8	90.8

Table 6: Ablation studies on the extremely long sequence experiments. Results are averaged over 3 runs.

Q-prompt Aggregation: Table 5 demonstrates the efficacy of the knowledge aggregation technique. In both the short and long task sequences, compared with the complete Q-prompt model (the fourth row), dropping the knowledge aggregation (the third row) leads to 0.8% and 1.1% accuracy drop in the short and long task sequences, respectively. In addition, in Fig. 2, we visualize the trained weight matrix \mathcal{W} to reflect the relevance of previously learned prompts to the current task. We can observe when learning the “sst2” task, the prompt from the “imdb” task contributes the most. This is because the two tasks are both for the movie review classification. The aggregation matrix uncovers their correlation and assigns more weights to the prompt of the “imdb” task. In contrast, for the “qnli” task, the aggregation matrix suggests an even contribution of each prompt in the queue. This is because all the tasks are of the Q&A classification.

Shared Prefix Prompt and MR: We conduct ablation studies to validate the efficacy of the shared prefix prompt and the MR regularization.

As shown in Table 5, by comparing the complete Q-prompt (the fourth row) and dropping the shared prefix prompt (the second row), we observe an accuracy drop of 0.9% and 1.2% in the short and long task sequences, respectively. This negative impact in the short sequence is weaker than that of the long task sequence. This is expected as the short task sequence does not utilize DQ-PCA to trim the Q-prompt, hence no information loss, which dilutes the effect of the shared prefix prompt. Furthermore, to evaluate the contribution of the MR regularization, we conduct the experiments on a long task sequence by setting $Q_{\text{size}} = 10$. Table 6 shows that dropping the MR regularization of the shared prefix prompt (from the third row to the second row) leads to a 1% accuracy drop. In Appendix D, we report the performance using different values of η for the MR regularization.

6 Conclusion

This paper introduces a new model-agnostic approach named Q-tuning, which can pave the way to achieving lifelong continual prompt tuning for present and future LMs with a rapid growth of parameters. In comparison with existing CL methods, Q-tuning maintains a low-cost prompt queue instead of storing a large number of task-specific parameters or saving old data samples for replay. Our extensive experiments demonstrate that Q-tuning outperforms existing continual learning, prompt tuning and continual prompt tuning methods on the standard CL benchmarks for text classification. In addition, we verify the effectiveness of Q-tuning on both short and long task sequences, including up to 70 tasks that mimic the case of lifelong learning.

Limitations: Although Q-tuning demonstrates a strong FKT capability, it does not enable the backward knowledge transfer as both the model and the previous Q-prompts are frozen during the learning of a new task. Besides, Q-tuning requires the task identities to be known at test time. To address the more challenging CL scenario when the task identities are undisclosed at test time, for task i , we can assign a trainable query key k^i to the corresponding Q-prompt Q^i and jointly train k^i to maximize the similarity between k^i and the feature of each sample x from task i . During test time, given an input x' with an unknown identity, we will first locate the Q-prompt that has the largest similarity between its key k^j and the input x' , and then we can use the retrieved Q-prompt Q^j to infer

x' . We will address this problem in our future work.

References

- Armen Aghajanyan, Sonal Gupta, and Luke Zettlemoyer. 2021. Intrinsic dimensionality explains the effectiveness of language model fine-tuning. In *Proceedings of the 59th Annual Meeting of the Association for Computational Linguistics and the 11th International Joint Conference on Natural Language Processing (Volume 1: Long Papers)*, pages 7319–7328.
- Cyprien de Masson Autume, Sebastian Ruder, Lingpeng Kong, and Dani Yogatama. 2019. Episodic memory in lifelong language learning. In *Proceedings of the 33rd International Conference on Neural Information Processing Systems*, pages 13132–13141.
- Jihwan Bang, Heesu Kim, Youngjoon Yoo, Jung-Woo Ha, and Jonghyun Choi. 2021. [Rainbow memory: Continual learning with a memory of diverse samples](#). In *IEEE Conference on Computer Vision and Pattern Recognition, CVPR 2021, virtual, June 19-25, 2021*, pages 8218–8227. Computer Vision Foundation / IEEE.
- David Barber and Felix Agakov. 2004. The im algorithm: a variational approach to information maximization. *Advances in neural information processing systems*, 16(320):201.
- Mohamed Ishmael Belghazi, Aristide Baratin, Sai Rajeshwar, Sherjil Ozair, Yoshua Bengio, Aaron Courville, and Devon Hjelm. 2018. Mutual information neural estimation. In *Proceedings of the 35th International Conference on Machine Learning*, volume 80 of *Proceedings of Machine Learning Research*, pages 531–540. PMLR.
- Tom Brown, Benjamin Mann, Nick Ryder, Melanie Subbiah, Jared D Kaplan, Prafulla Dhariwal, Arvind Neelakantan, Pranav Shyam, Girish Sastry, Amanda Askell, et al. 2020. Language models are few-shot learners. *Advances in neural information processing systems*, 33:1877–1901.
- Inigo Casanueva, Tadas Temvinas, Daniela Gerz, Matthew Henderson, and Ivan Vulic. 2020. Efficient intent detection with dual sentence encoders. In *Proceedings of the 2nd Workshop on Natural Language Processing for Conversational AI*, pages 38–45.
- Arslan Chaudhry, Marc’Aurelio Ranzato, Marcus Rohrbach, and Mohamed Elhoseiny. 2018. Efficient lifelong learning with a-gem. In *International Conference on Learning Representations*.
- Jacob Devlin, Ming-Wei Chang, Kenton Lee, and Kristina Toutanova. 2018. Bert: Pre-training of deep bidirectional transformers for language understanding. *arXiv preprint arXiv:1810.04805*.

- Beyza Ermis, Giovanni Zappella, Martin Wistuba, Aditya Rawal, and Cedric Archambeau. 2022. Memory efficient continual learning with transformers. *Advances in Neural Information Processing Systems*, 35:10629–10642.
- Jinmiao Fu, Shaoyuan Xu, Huidong Liu, Yang Liu, Ning Xie, Chien-Chih Wang, Jia Liu, Yi Sun, and Bryan Wang. 2022. [Cma-clip: Cross-modality attention clip for text-image classification](#). In *2022 IEEE International Conference on Image Processing (ICIP)*, pages 2846–2850.
- Yuxian Gu, Xu Han, Zhiyuan Liu, and Minlie Huang. 2022. [PPT: Pre-trained prompt tuning for few-shot learning](#). In *Proceedings of the 60th Annual Meeting of the Association for Computational Linguistics (Volume 1: Long Papers)*, pages 8410–8423, Dublin, Ireland. Association for Computational Linguistics.
- Geoffrey Hinton, Oriol Vinyals, and Jeff Dean. 2015. Distilling the knowledge in a neural network. *arXiv preprint arXiv:1503.02531*.
- Jean-Baptiste Hiriart-Urruty and Claude Lemaréchal. 2004. *Fundamentals of convex analysis*. Springer Science & Business Media.
- R Devon Hjelm, Alex Fedorov, Samuel Lavoie-Marchildon, Karan Grewal, Phil Bachman, Adam Trischler, and Yoshua Bengio. 2018. Learning deep representations by mutual information estimation and maximization. In *International Conference on Learning Representations*.
- Yufan Huang, Yanzhe Zhang, Jiaao Chen, Xuezhi Wang, and Diyi Yang. 2021. Continual learning for text classification with information disentanglement based regularization. *arXiv preprint arXiv:2104.05489*.
- Menglin Jia, Luming Tang, Bor-Chun Chen, Claire Cardie, Serge Belongie, Bharath Hariharan, and Ser-Nam Lim. 2022. Visual prompt tuning. In *European Conference on Computer Vision*, pages 709–727. Springer.
- Qinjin Jia, Yang Liu, Daoping Wu, Shaoyuan Xu, Huidong Liu, Jinmiao Fu, Roland Vollgraf, and Bryan Wang. 2023. [KG-FLIP: Knowledge-guided fashion-domain language-image pre-training for E-commerce](#). In *Proceedings of the 61st Annual Meeting of the Association for Computational Linguistics (Volume 5: Industry Track)*, pages 81–88, Toronto, Canada. Association for Computational Linguistics.
- Yang Jiao, Ning Xie, Yan Gao, Chien-Chih Wang, and Yi Sun. 2022. Fine-grained fashion representation learning by online deep clustering. In *European Conference on Computer Vision*, pages 19–35. Springer.
- Zixuan Ke, Bing Liu, Nianzu Ma, Hu Xu, and Lei Shu. 2021. Achieving forgetting prevention and knowledge transfer in continual learning. *Advances in Neural Information Processing Systems*, 34:22443–22456.
- Ronald Kemker, Marc McClure, Angelina Abitino, Tyler Hayes, and Christopher Kanan. 2018. Measuring catastrophic forgetting in neural networks. In *Proceedings of the AAAI conference on artificial intelligence*, volume 32.
- James Kirkpatrick, Razvan Pascanu, Neil Rabinowitz, Joel Veness, Guillaume Desjardins, Andrei A Rusu, Kieran Milan, John Quan, Tiago Ramalho, Agnieszka Grabska-Barwinska, et al. 2017. Overcoming catastrophic forgetting in neural networks. *Proceedings of the national academy of sciences*, 114(13):3521–3526.
- Brian Lester, Rami Al-Rfou, and Noah Constant. 2021. [The power of scale for parameter-efficient prompt tuning](#). In *Proceedings of the 2021 Conference on Empirical Methods in Natural Language Processing*, pages 3045–3059, Online and Punta Cana, Dominican Republic. Association for Computational Linguistics.
- Xiang Lisa Li and Percy Liang. 2021. Prefix-tuning: Optimizing continuous prompts for generation. In *Proceedings of the 59th Annual Meeting of the Association for Computational Linguistics and the 11th International Joint Conference on Natural Language Processing (Volume 1: Long Papers)*, pages 4582–4597.
- Sen Lin, Li Yang, Deliang Fan, and Junshan Zhang. 2022. [Trgp: Trust region gradient projection for continual learning](#). *arXiv preprint arXiv:2202.02931*.
- Pengfei Liu, Weizhe Yuan, Jinlan Fu, Zhengbao Jiang, Hiroaki Hayashi, and Graham Neubig. 2023. Pre-train, prompt, and predict: A systematic survey of prompting methods in natural language processing. *ACM Computing Surveys*, 55(9):1–35.
- Xiao Liu, Kaixuan Ji, Yicheng Fu, Weng Tam, Zhengxiao Du, Zhilin Yang, and Jie Tang. 2022. P-tuning: Prompt tuning can be comparable to fine-tuning across scales and tasks. In *Proceedings of the 60th Annual Meeting of the Association for Computational Linguistics (Volume 2: Short Papers)*, pages 61–68.
- David Lopez-Paz and Marc’Aurelio Ranzato. 2017. Gradient episodic memory for continual learning. *Advances in neural information processing systems*, 30.
- Andrew Maas, Raymond E Daly, Peter T Pham, Dan Huang, Andrew Y Ng, and Christopher Potts. 2011. Learning word vectors for sentiment analysis. In *Proceedings of the 49th annual meeting of the association for computational linguistics: Human language technologies*, pages 142–150.
- Rafael Müller, Simon Kornblith, and Geoffrey E Hinton. 2019. When does label smoothing help? *Advances in neural information processing systems*, 32.
- XuanLong Nguyen, Martin J. Wainwright, and Michael I. Jordan. 2010. [Estimating divergence functionals and the likelihood ratio by convex risk minimization](#). *IEEE Transactions on Information Theory*, 56(11):5847–5861.

- Sebastian Nowozin, Botond Cseke, and Ryota Tomioka. 2016. f-gan: Training generative neural samplers using variational divergence minimization. *Advances in neural information processing systems*, 29.
- OpenAI. 2023. [Gpt-4 technical report](#).
- Ben Poole, Sherjil Ozair, Aaron Van Den Oord, Alex Alemi, and George Tucker. 2019. On variational bounds of mutual information. In *International Conference on Machine Learning*, pages 5171–5180. PMLR.
- Chengwei Qin and Shafiq Joty. 2021. Lfpt5: A unified framework for lifelong few-shot language learning based on prompt tuning of t5. In *International Conference on Learning Representations*.
- Colin Raffel, Noam Shazeer, Adam Roberts, Katherine Lee, Sharan Narang, Michael Matena, Yanqi Zhou, Wei Li, and Peter J Liu. 2020. Exploring the limits of transfer learning with a unified text-to-text transformer. *The Journal of Machine Learning Research*, 21(1):5485–5551.
- Anastasia Razdaibiedina, Yuning Mao, Rui Hou, Madihan Khabsa, Mike Lewis, and Amjad Almahairi. 2023. Progressive prompts: Continual learning for language models. In *International Conference on Learning Representations*.
- Andrei A Rusu, Neil C Rabinowitz, Guillaume Desjardins, Hubert Soyer, James Kirkpatrick, Koray Kavukcuoglu, Razvan Pascanu, and Raia Hadsell. 2016. Progressive neural networks. *arXiv preprint arXiv:1606.04671*.
- Elvis Saravia, Hsien-Chi Toby Liu, Yen-Hao Huang, Junlin Wu, and Yi-Shin Chen. 2018. [CARER: Contextualized affect representations for emotion recognition](#). In *Proceedings of the 2018 Conference on Empirical Methods in Natural Language Processing*, pages 3687–3697, Brussels, Belgium. Association for Computational Linguistics.
- Jonathan Schwarz, Wojciech Czarnecki, Jelena Luketina, Agnieszka Grabska-Barwinska, Yee Whye Teh, Razvan Pascanu, and Raia Hadsell. 2018. Progress & compress: A scalable framework for continual learning. In *International conference on machine learning*, pages 4528–4537. PMLR.
- Hanul Shin, Jung Kwon Lee, Jaehong Kim, and Jiwon Kim. 2017. Continual learning with deep generative replay. In *Proceedings of the 31st International Conference on Neural Information Processing Systems, NIPS’17*, page 2994–3003, Red Hook, NY, USA. Curran Associates Inc.
- Jonathon Shlens. 2014. A tutorial on principal component analysis. *arXiv preprint arXiv:1404.1100*.
- James Seale Smith, Leonid Karlinsky, Vyshnavi Gutta, Paola Cascante-Bonilla, Donghyun Kim, Assaf Arbelle, Rameswar Panda, Rogerio Feris, and Zsolt Kira. 2023. Coda-prompt: Continual decomposed attention-based prompting for rehearsal-free continual learning. In *Proceedings of the IEEE/CVF Conference on Computer Vision and Pattern Recognition*, pages 11909–11919.
- Romal Thoppilan, Daniel De Freitas, Jamie Hall, Noam Shazeer, Apoorv Kulshreshtha, Heng-Tze Cheng, Alicia Jin, Taylor Bos, Leslie Baker, Yu Du, et al. 2022. Lamda: Language models for dialog applications. *arXiv preprint arXiv:2201.08239*.
- Yonglong Tian, Dilip Krishnan, and Phillip Isola. 2019. Contrastive representation distillation. *arXiv preprint arXiv:1910.10699*.
- Alex Wang, Yada Pruksachatkun, Nikita Nangia, Amanpreet Singh, Julian Michael, Felix Hill, Omer Levy, and Samuel Bowman. 2019. Superglue: A stickier benchmark for general-purpose language understanding systems. *Advances in neural information processing systems*, 32.
- Alex Wang, Amanpreet Singh, Julian Michael, Felix Hill, Omer Levy, and Samuel R Bowman. 2018. Glue: A multi-task benchmark and analysis platform for natural language understanding. In *International Conference on Learning Representations*.
- Yabin Wang, Zhiwu Huang, and Xiaopeng Hong. 2022a. [S-prompts learning with pre-trained transformers: An occam’s razor for domain incremental learning](#). *ArXiv*, abs/2207.12819.
- Zhen Wang, Rameswar Panda, Leonid Karlinsky, Rogerio Feris, Huan Sun, and Yoon Kim. 2023. Multitask prompt tuning enables parameter-efficient transfer learning. *International Conference on Learning Representations (ICLR)*.
- Zifeng Wang, Zizhao Zhang, Sayna Ebrahimi, Ruoxi Sun, Han Zhang, Chen-Yu Lee, Xiaoqi Ren, Guolong Su, Vincent Perot, Jennifer Dy, et al. 2022b. Dual-prompt: Complementary prompting for rehearsal-free continual learning. In *European Conference on Computer Vision*, pages 631–648. Springer.
- Zirui Wang, Sanket Vaibhav Mehta, Barnabás Póczos, and Jaime G Carbonell. 2020. Efficient meta lifelong-learning with limited memory. In *Proceedings of the 2020 Conference on Empirical Methods in Natural Language Processing (EMNLP)*, pages 535–548.
- Wenpeng Yin, Jia Li, and Caiming Xiong. 2022. Continint: Continual learning from task instructions. In *Proceedings of the 60th Annual Meeting of the Association for Computational Linguistics (Volume 1: Long Papers)*, pages 3062–3072.
- Jaehong Yoon, Saehoon Kim, Eunho Yang, and Sung Ju Hwang. 2020. Scalable and order-robust continual learning with additive parameter decomposition. In *Eighth International Conference on Learning Representations, ICLR 2020*. ICLR.

- Jaehong Yoon, Eunho Yang, Jeongtae Lee, and Sung Ju Hwang. 2018. Lifelong learning with dynamically expandable networks. In *6th International Conference on Learning Representations, ICLR 2018*. International Conference on Learning Representations, ICLR.
- Friedemann Zenke, Ben Poole, and Surya Ganguli. 2017. Continual learning through synaptic intelligence. In *International conference on machine learning*, pages 3987–3995. PMLR.
- Xiang Zhang, Junbo Zhao, and Yann LeCun. 2015. Character-level convolutional networks for text classification. *Advances in neural information processing systems*, 28.
- Qi Zhu, Bing Li, Fei Mi, Xiaoyan Zhu, and Minlie Huang. 2022. Continual prompt tuning for dialog state tracking. *arXiv preprint arXiv:2203.06654*.

Appendix

A Q-tuning Algorithm

Algorithm 1 Q-tuning Algorithm

Input: Continually increased task set \mathcal{T} , Q-prompt \mathcal{Q} with a maximum capacity C , fixed pretrained model $\theta_{\mathcal{M}}$, aggregation matrix \mathcal{W} for \mathcal{Q} , shared prefix prompt $\theta_{\mathcal{P}^*}$, memory factor η .

Initialize: $\mathcal{Q}^1 = \{\}$, randomly initialized $\theta_{\mathcal{P}^*}^1$ and $\theta_{\mathcal{P}}^1$, initialized \mathcal{W}^1 with an identity matrix.

for continually coming task $i = 1, 2, \dots$ **do**

if $i > C$ **then**

$\mathcal{Q} \leftarrow \text{PCA-DQ}(\mathcal{Q})$ // De-Q (Eq.(5))

else

$\mathcal{Q} \leftarrow \mathcal{Q} \oplus \theta_{\mathcal{P}}^i$ // En-Q

end if

for each batch sample from \mathcal{T}^i 's dataset **do**

$\theta_{\mathcal{P}}^i \leftarrow \theta_{\mathcal{P}}^i + \nabla_{\theta_{\mathcal{P}}^i} \mathcal{L}_{\mathcal{Q}}(\theta_{\mathcal{P}^*}^i, \theta_{\mathcal{P}}^i, \mathcal{W}^i)$

$\mathcal{W}^i \leftarrow \mathcal{W}^i + \nabla_{\mathcal{W}^i} \mathcal{L}_{\mathcal{Q}}(\theta_{\mathcal{P}^*}^i, \theta_{\mathcal{P}}^i, \mathcal{W}^i)$

if $i=1$ **then**

$\theta_{\mathcal{P}^*}^i \leftarrow \theta_{\mathcal{P}^*}^i + \nabla_{\theta_{\mathcal{P}^*}^i} \mathcal{L}_{\mathcal{Q}}(\theta_{\mathcal{P}^*}^i, \theta_{\mathcal{P}}^i, \mathcal{W}^i)$

else if $i > C$ **then**

$\theta_{\mathcal{P}^*}^i \leftarrow \theta_{\mathcal{P}^*}^i + \nabla_{\theta_{\mathcal{P}^*}^i} [\mathcal{L}_{\mathcal{Q}}(\theta_{\mathcal{P}^*}^i, \theta_{\mathcal{P}}^i, \mathcal{W}^i) + \eta \mathcal{L}_{\text{MR}}(\theta_{\mathcal{P}^*}^i)]$

end if

end for

end for

B Mutual Information Estimation

Proposition 1. Let $p(x)$ and $p(y)$ represent two random variables, their mutual information satisfies

$$\begin{aligned} I(p(x); p(y)) &:= \mathcal{D}_{\text{JSD}}(\mathbf{J} \parallel \mathbf{M}) \\ &\geq \mathbb{E}_{z \sim \mathbf{J}} [-\sigma(-\mathcal{F}_{\omega}(z))] - \mathbb{E}_{z' \sim \mathbf{M}} [\sigma(\mathcal{F}_{\omega}(z'))] \end{aligned} \quad (11)$$

where the joint $\mathbf{J} = p(x, y)$, $\mathbf{M} = p(x)p(y)$ is the product of the marginals, $\sigma(t) = \log(1 + e^t)$, and \mathcal{F} belongs to an arbitrary class of functions that can map $\mathbf{J} \rightarrow \mathbb{R}$ and $\mathbf{M} \rightarrow \mathbb{R}$.

Proof. According to the variational estimation of f -divergences (Nguyen et al., 2010), we have

$$\begin{aligned} \mathcal{D}_f(\mathbf{P} \parallel \mathbf{Q}) &= \int q(x) \sup_{t \in \text{dom}_{g^*}} t \frac{p(x)}{q(x)} - g^*(t) dx \\ &\geq \sup_{\mathcal{V} \in \mathcal{F}} \left(\int p(x) \mathcal{V}(x) dx - \int q(x) g^*(\mathcal{V}(x)) dx \right) \\ &= \sup_{\mathcal{V} \in \mathcal{F}} (\mathbb{E}_{x \sim \mathbf{P}} [\mathcal{V}(x)] - \mathbb{E}_{x \sim \mathbf{Q}} [g^*(\mathcal{V}(x))]) \end{aligned} \quad (12)$$

where the function g^* is a convex conjugate function (Hiriart-Urruty and Lemaréchal, 2004; Nowozin et al., 2016) of a convex, lower-semicontinuous function. The function g^* is defined as

$$g^*(t) = \sup_{u \in \text{dom}_f} \{ut - f(u)\} \quad (13)$$

We parameterize \mathcal{V} using a neural network with parameters w and write it as \mathcal{V}_{ω} . We assume the form of the function $\mathcal{V}_{\omega} = g_f(\mathcal{F}_{\omega}(x))$. Given two probability distributions $\mathbf{J} = p(x, y)$ and $\mathbf{M} = p(x)p(y)$, their f -divergence satisfies:

$$\begin{aligned} \mathcal{D}_f(\mathbf{J} \parallel \mathbf{M}) &= \sup_{\mathcal{F}_{\omega}} (\mathbb{E}_{z \sim \mathbf{J}} [g_f(\mathcal{F}_{\omega}(z))] \\ &\quad - \mathbb{E}_{z' \sim \mathbf{M}} [g^*(g_f(\mathcal{F}_{\omega}(z')))]) \end{aligned} \quad (14)$$

where g_f is an activation function specific to the f -divergence used. Table 7 provides the commonly used g_f and the convex conjugate function g^* . According to this table, for the JSD based divergence, we have $g_f(x) = \log(2) - \log(1 + \exp(-x))$ and $g^*(x) = -\log(2 - \exp(x))$. By substituting them into Eq. (14), we have

$$\begin{aligned} \mathbb{E}_{z \sim \mathbf{J}} [g_f(\mathcal{F}_{\omega}(z))] &= \mathbb{E} [\log 2 - \log(1 + \exp(-\mathcal{F}_{\omega}(z)))] \\ &= \mathbb{E}_{z \sim \mathbf{J}} [\log 2 - \sigma(-\mathcal{F}_{\omega}(z))] \end{aligned} \quad (15)$$

$$\begin{aligned} \mathbb{E}_{z' \sim \mathbf{M}} [g^*(g_f(\mathcal{F}_{\omega}(z')))] &= \mathbb{E}_{z' \sim \mathbf{M}} [-\log(2 - \exp^{\log 2 - \log(1 + \exp(-\mathcal{F}_{\omega}(z'))}))] \\ &= \mathbb{E}_{z' \sim \mathbf{M}} [-\log(2 - 2(1 + \exp(-\mathcal{F}_{\omega}(z')))^{-1})] \\ &= \mathbb{E}_{z' \sim \mathbf{M}} \left[-\log\left(2 \frac{\exp(-\mathcal{F}_{\omega}(z'))}{1 + \exp(-\mathcal{F}_{\omega}(z'))}\right) \right] \\ &= \mathbb{E}_{z' \sim \mathbf{M}} \left[-\log\left(\frac{2}{\exp(\mathcal{F}_{\omega}(z')) + 1}\right) \right] \\ &= \mathbb{E}_{z' \sim \mathbf{M}} [-\log 2 - \log(\exp(\mathcal{F}_{\omega}(z')) + 1)] \\ &= \mathbb{E}_{z' \sim \mathbf{M}} [-\log 2 + \sigma(\mathcal{F}_{\omega}(z'))] \end{aligned} \quad (16)$$

Combining Eq. (15) and Eq. (16), we can rewrite Eq. (14) as a JSD-divergence based form:

$$\begin{aligned} \mathcal{D}_{\text{JSD}}(\mathbf{J} \parallel \mathbf{M}) &= \sup_{\mathcal{F}_{\omega}} (\mathbb{E}_{z \sim \mathbf{J}} [\log 2] + \mathbb{E}_{z \sim \mathbf{J}} [-\sigma(-\mathcal{F}_{\omega}(z))] \\ &\quad + \mathbb{E}_{z' \sim \mathbf{M}} [\log 2] - \mathbb{E}_{z' \sim \mathbf{M}} [\sigma(\mathcal{F}_{\omega}(z'))]) \\ &\geq \mathbb{E}_{z \sim \mathbf{J}} [-\sigma(-\mathcal{F}_{\omega}(z))] - \mathbb{E}_{z' \sim \mathbf{M}} [\sigma(\mathcal{F}_{\omega}(z'))] \end{aligned} \quad (17)$$

□

C More Implementation Details

C.1 Datasets and Metrics

We use 21 public datasets, of which 15 datasets are the same as ProgPrompt (Razdaibiedina et al., 2023) for our experiments. Table 8 reports the details of the 21 datasets, along with their evaluation metrics. Overall, we use datasets from CL benchmark (Zhang et al., 2015), GLUE (Wang et al., 2018) and SuperGLUE (Wang et al., 2019) benchmarks, and IMDB movie reviews dataset. We use the Banking77 dataset (Casanueva et al., 2020) and Emotion dataset (Saravia et al., 2018) for the extremely long 70-task experiments. Following the

Name	Output activation g_f	dom_{g^*}	Conjugate $g^*(t)$
Kullback-Leibler (KL)	v	\mathbb{R}	$\exp(t - 1)$
Reverse KL	$-\exp(-v)$	\mathbb{R}_-	$-1 - \log(-t)$
Pearson χ^2	v	\mathbb{R}	$\frac{1}{4}t^2 + t$
Square Hellinger	$1 - \exp(-v)$	$t < 1$	$\frac{t}{1-t}$
Jensen-Shannon	$\log(2) - \log(1 + \exp(-v))$	$t < \log(2)$	$-\log(2 - \exp(t))$

Table 7: Recommended final layer activation functions and their conjugate functions. This table comes from Nowozin et al. (2016).

common practice, for tasks that have two evaluation metrics, we use the average of the two as the final performance metric.

To mimic the life-long learning, we add WNLI, COLA, and QNLI from the GLUE benchmark, WSC from the SuperGLUE benchmark, the Banking77 dataset (Casanueva et al., 2020) and the Emotion dataset (Saravia et al., 2018) to form an extremely long sequence including 70 tasks. In the 70-task experiments, we split the DBpedia set into 7 **disjoint** tasks, the Yahoo set into 5 **disjoint** tasks, and the Banking77 set into 38 **disjoint** tasks (removing 1 class), and the Emotion dataset into 3 **disjoint** tasks, where each task has two 2 classes. These divided 53 subsets plus the rest 17 datasets form the final 70-task dataset. Following (Razdaibiedina et al., 2023), for each task, we randomly select 500 samples per class from the training set for validation, and use early stopping according to the validation accuracy on all seen tasks.

C.2 Task sequence orders

We report the task orders used in our experiments across the T5 and BERT models in Table 9 below, where Orders 1-10 are the same as ProgPrompt (Razdaibiedina et al., 2023). The Orders 11-13 are created by **randomly permuting** the collected 70 disjoint datasets to mimic the lifelong learning of continuously incoming unseen tasks.

C.3 Implementation and Experiment Details

More Details of the Methods for Comparison

Following (Razdaibiedina et al., 2023), we consider 11 baseline methods for comparison with the proposed Q-tuning:

- **Per-task Finetune** separately tunes the whole model for each task. We use this type of method as a baseline in the short-sequence benchmark experiments.
- **Continual Finetune** (Wang et al., 2020; Huang et al., 2021) continually tunes the whole model

on a sequence of tasks without adding any regularization or replaying data from the previous tasks.

- **Prompt Tuning** (Qin and Joty, 2021; Lester et al., 2021) sequentially trains a shared soft prompt across all tasks, while freezing the pre-trained model.
- **Data Replay** finetunes the whole model for new tasks while replaying samples from previous tasks to prevent the CF problem.
- **EWC** (Kirkpatrick et al., 2017) finetunes the whole model using a regularization loss which penalizes updating parameters that could disturb the previously learned tasks.
- **A-GEM** (Chaudhry et al., 2018) retrieves examples from old tasks and restricts the gradients to update the model when learning new tasks.
- **LFPT5** (Qin and Joty, 2021) continuously trains a soft prompt that learns the tasks while generating samples for experience replay.
- **MBPA++** (Autume et al., 2019) uses an episodic memory to augment BERT by storing all seen examples.
- **IDBR** (Huang et al., 2021) continuously trains the whole model by using data replay and a regularization loss. It adopts sentence representation disentanglement in task-specific and task-generic spaces, achieving SOTA on the CL benchmark with BERT.
- **Per-task Prompt** (Lester et al., 2021) trains a separate soft prompt for each task while keeping the original model frozen. This type of method naturally eliminates the CF problem, because separately tuned prompts will not change when new tasks are learned. However, this independent prompt tuning setup cannot achieve forward knowledge transfer.

Table 8: The details of 21 datasets used in our experiments. NLI denotes natural language inference, QA denotes questions and answers task, and EM denotes exact match scoring. The first five tasks are used to form the standard CL benchmark, all other tasks are used in our long-sequence experiments.

Dataset name	Category	Task	Domain	Metric	Classes
1. YP	CL benchmark	sentiment analysis	YP reviews	accuracy	5
2. Amazon	CL benchmark	sentiment analysis	Amazon reviews	accuracy	5
3. DBpedia	CL benchmark	topic classification	Wikipedia	accuracy	14
4. Yahoo	CL benchmark	QA	Yahoo Q&A	accuracy	10
5. AG News	CL benchmark	topic classification	news	accuracy	4
6. MNLI	GLUE	NLI	various	accuracy	3
7. QQP	GLUE	paraphrase detection	Quora	accuracy & F1	2
8. RTE	GLUE	NLI	news, Wikipedia	accuracy	2
9. SST2	GLUE	sentiment analysis	movie reviews	accuracy	2
10. WiC	SuperGLUE	word sense disambiguation	lexical databases	accuracy	2
11. CB	SuperGLUE	NLI	various	accuracy	2
12. COPA	SuperGLUE	QA	blogs, encyclopedia	accuracy	2
13. BoolQ	SuperGLUE	boolean QA	Wikipedia	accuracy	2
14. MultiRC	SuperGLUE	QA	various	F1 & EM	2
15. IMDB	Other	sentiment analysis	movie reviews	accuracy	2
16. WNLI	GLUE	NLI	various	accuracy	2
17. COLA	GLUE	NLI	books, journal articles	accuracy	2
18. QNLI	GLUE	QA	Wikipedia	accuracy	2
19. WSC	SuperGLUE	NLI	various	accuracy	2
20. Banking77	Other	intent detection	banking	accuracy	77
21. Emotion	Other	emotion detection	Twitter	accuracy	6

- **ProgPrompt** (Razdaibiedina et al., 2023) trains a progressively increased prompt list to achieve the forward knowledge transfer and resist the CF problem using prompt tuning without relying on data replay. Current SOTA on continual prompt tuning benchmarks with T5 and BERT.

Implementation Details We use PyTorch and HuggingFace Transformers library for our implementation. For the standard CL benchmark, we use official datasets provided by Zhang et al. (2015), following Autume et al. (2019); Zhang et al. (2015). We use HuggingFace datasets (<https://github.com/huggingface/datasets>) to download data for GLUE tasks (Wang et al., 2018), SuperGLUE tasks (Wang et al., 2019) tasks, IMDB movie reviews dataset (Maas et al., 2011), Banking77 dataset (Casanueva et al., 2020), and Emotion dataset (Saravia et al., 2018), which we use for long-sequence CL experiments, life-long learning experiments and ablation studies. Following previous studies (Autume et al., 2019; Razdaibiedina et al., 2023), for CL experiments, for each dataset, we use the available validation set as a test set (since test data is not available), and hold out 500 samples from the train set to construct the validation set. For our ablation studies, we report the maximal validation set performance.

We use the Adam optimizer and set the batch size to 8 for all the experiments. Following (Razdaibiedina et al., 2023), we train each prompt between

20 and 300 epochs, depending on the number of data points. We use the prompt checkpoints with the best validation set score as our final prompts. Prompts are initialized from randomly sampled tokens as in Lester et al. (2021), hyperparameters are shown in the Table 10.

The mutual information maximization can be approximated by maximizing its variational lower bound (Barber and Agakov, 2004; Poole et al., 2019) defined by Eq. (7). But this variational approximation requires extra costly computation to optimize the discriminator \mathcal{F}_w . We empirically find a KL-divergence based loss can go for the same goal, which is also verified by (Müller et al., 2019; Tian et al., 2019). The KL-divergence based MR loss between the new memory and the old memory is defined as follows:

$$\mathcal{L}_{\text{MR}} = \sum_{i \in |\mathcal{T}|} \sum_{(\mathbf{x}^i, \mathbf{y}^i) \in \mathcal{T}^i} D_{\text{KL}}(p(\mathbf{y}^i | \mathbf{x}^i; \theta_{\mathcal{M}}, \theta_{\mathcal{P}^*}^i) \| p(\mathbf{y}^i | \mathbf{x}^i; \theta_{\mathcal{M}}, \mathcal{W}^{i-1} \circ [\theta_{\mathcal{P}^*}^{i-1}, \mathcal{Q}^{i-1}])), \quad (18)$$

where only the shared prefix prompt $\theta_{\mathcal{P}^*}^i$ is trainable. This MR regularization loss does not require training an extra discriminator network, achieving the same objective as knowledge distillation (Hinton et al., 2015).

For all the CL experiments, we use early stopping as in Huang et al. (2021), to save model checkpoint based on the best validation performance on

Order	Model	Task Sequence
1	T5	db → amazon → yahoo → ag
2	T5	db → amazon → ag → yahoo
3	T5	yahoo → amazon → ag → db
4	BERT	ag → yp → amazon → yahoo → db
5	BERT	yp → yahoo → amazon → db → ag
6	BERT	db → yahoo → ag → amazon → yp
7	BERT	yp → ag → db → amazon → yahoo
8	T5, BERT	mnli → cb → wic → copa → qqp → boolq → rte → imdb → yp → amazon → sst2 → dbpedia → ag → multirc → yahoo
9	T5, BERT	multirc → boolq → wic → mnli → cb → copa → qqp → rte → imdb → sst2 → dbpedia → ag → yp → amazon → yahoo
10	T5, BERT	yp → amazon → mnli → cb → copa → qqp → rte → imdb → sst2 → dbpedia → ag → yahoo → multirc → boolq → wic
11	T5	wsc → banking77-19 → banking77-9 → banking77-8 → banking77-25 → yahoo-1 → banking77-34 → banking77-3 → banking77-23 → cb → banking77-7 → banking77-35 → banking77-13 → imdb → banking77-12 → banking77-17 → multirc → banking77-14 → emotion-0 → banking77-22 → yp → dbpedia-14-5 → banking77-30 → banking77-1 → banking77-15 → boolq → banking77-20 → banking77-21 → dbpedia-14-2 → qnli → banking77-31 → banking77-29 → emotion-2 → yahoo-3 → dbpedia-14-1 → banking77-32 → banking77-0 → rte → ag-news → dbpedia-14-4 → banking77-2 → yahoo-4 → banking77-11 → banking77-37 → banking77-27 → sst2 → banking77-33 → copa → banking77-5 → dbpedia-14-0 → wic → qqp → banking77-26 → yahoo-2 → banking77-10 → banking77-36 → banking77-4 → emotion-1 → dbpedia-14-3 → amazon → banking77-28 → banking77-16 → banking77-24 → mnli → cola → wnli → banking77-18 → banking77-6 → dbpedia-14-6 → yahoo-0
12	T5	banking77-29 → yp → banking77-30 → banking77-26 → banking77-20 → yahoo-2 → amazon → dbpedia-14-2 → banking77-24 → yahoo-3 → banking77-22 → banking77-16 → yahoo-0 → dbpedia-14-1 → emotion-2 → dbpedia-14-4 → dbpedia-14-6 → wic → banking77-23 → banking77-14 → banking77-18 → yahoo-4 → banking77-5 → banking77-0 → banking77-13 → cb → banking77-35 → rte → banking77-4 → dbpedia-14-3 → banking77-1 → banking77-9 → banking77-15 → banking77-3 → banking77-6 → banking77-21 → mnli → banking77-2 → yahoo-1 → boolq → banking77-10 → banking77-25 → banking77-37 → banking77-17 → qqp → banking77-28 → wnli → banking77-8 → banking77-31 → dbpedia-14-0 → banking77-11 → banking77-27 → banking77-7 → multirc → banking77-33 → banking77-12 → imdb → copa → banking77-19 → cola → banking77-34 → sst2 → emotion-0 → wsc → qnli → emotion-1 → banking77-32 → dbpedia-14-5 → ag-news → banking77-36
13	T5	yahoo-2 → copa → banking77-22 → emotion-0 → banking77-1 → emotion-1 → yahoo-0 → banking77-32 → banking77-37 → dbpedia-14-0 → banking77-3 → qnli → multirc → banking77-0 → dbpedia-14-3 → ag-news → banking77-10 → imdb → banking77-5 → banking77-15 → banking77-16 → wnli → banking77-36 → wsc → banking77-13 → banking77-19 → amazon → banking77-29 → banking77-33 → boolq → banking77-28 → yahoo-1 → yp → banking77-14 → emotion-2 → mnli → banking77-7 → banking77-21 → banking77-30 → banking77-4 → banking77-9 → banking77-35 → dbpedia-14-5 → banking77-26 → cola → qqp → yahoo-3 → dbpedia-14-6 → wic → banking77-25 → banking77-31 → banking77-17 → banking77-23 → banking77-8 → cb → banking77-6 → dbpedia-14-2 → banking77-20 → dbpedia-14-1 → yahoo-4 → banking77-18 → banking77-2 → banking77-34 → banking77-12 → dbpedia-14-4 → banking77-27 → rte → sst2 → banking77-24 → banking77-11

Table 9: Thirteen different orders of task sequences used for continual learning experiments. Orders 1-7 correspond to the standard CL benchmarks adopted by prior works (Razdaibiedina et al., 2023) for short-sequence experiments. Orders 8-10 are long-sequence orders spanning 15 tasks. Orders 11-13 are our customized extremely long sequences, where the tasks are **randomly permuted**. In these extremely long cases, existing techniques such as the SOTA, ProgPrompt (Razdaibiedina et al., 2023), cannot cope with these long tasks, due to the quadratic growing training and inference costs.

Hyperparameter ↓ Num. samples →	Short-sequence benchmark			Long-sequence benchmark		
	16	200	1000	20	200	1000
T5-large Model						
Epochs	300	150	20	300	150	20
Learning rate	0.3	0.3	0.3	0.3	0.3	0.3
Length of shared prompt θ_{P^*}	10	10	10	10	10	10
Length of each prompt in \mathcal{Q}	10	10	10	10	10	10
Memory factor η	0.001	0.001	0.001	0.01	0.01	0.01
BERT-base Model						
Epochs	300	150	40	300	150	40
Learning rate	0.0001	0.0001	0.0001	0.0001	0.0001	0.0001
Length of shared prompt θ_{P^*}	10	10	10	5	5	5
Length of each prompt in \mathcal{Q}	10	10	10	5	5	5
Memory factor η	0.001	0.001	0.001	0.01	0.01	0.01

Table 10: Hyperparameters used for Q-tuning across different CL experiments.

Sequence	Method			T5-large Results											
	Q-prompt (Num. samples →)	Aggregation	θ_{P^*}	Order1			Order2			Order3			Average		
				16	200	1000	16	200	1000	16	200	1000	16	200	1000
Short	✓			74.1	80.0	79.6	74.2	79.5	79.9	75.3	79.8	80.1	74.5	79.8	79.8
	✓	✓		74.9	80.9	80.4	75.1	80.6	80.1	75.6	81.1	80.8	75.2	80.9	80.4
	✓		✓	75.0	80.7	81.6	74.6	80.7	80.7	75.7	80.4	80.6	75.1	80.6	80.9
	✓	✓	✓	75.8	81.2	82.3	75.8	81.1	82.2	76.9	81.1	81.1	76.2	81.2	81.9

Sequence	Method			T5-large Results											
	Q-prompt (Num. samples →)	Aggregation	θ_{P^*}	Order8			Order9			Order10			Average		
				20	200	1000	20	200	1000	20	200	1000	20	200	1000
Long	✓			76.3	81.6	81.0	76.9	80.6	80.5	76.7	80.1	80.9	76.7	80.8	80.8
	✓	✓		77.1	81.6	82.1	77.4	81.7	81.9	77.2	80.2	82.4	77.2	81.1	82.1
	✓		✓	77.4	81.7	82.5	77.9	80.9	82.5	77.1	80.7	82.0	77.4	81.1	82.3
	✓	✓	✓	78.3	82.4	83.5	79.7	82.1	83.3	78.7	81.4	83.1	78.9	81.9	83.3

Table 11: More details of the ablation study results on each order reported in Table 5. For the long-sequence experiments, we set the queue size to 10. All results are averaged over 3 runs.

the current task. We report test set performance after training on all tasks as our final metric. For SuperGLUE experiments, we report maximal validation set performance over the course of training as in Lester et al. (2021). We measure the validation performance after every epoch and use metrics described in Appendix C.1. We use the same hyperparameter settings for all prompt-based approaches (Q-tuning, Progressive Prompts, per-task prompt) as in (Razdaibiedina et al., 2023).

MLP-based prompt We follow Razdaibiedina et al. (2023) by setting a two-layer MLP for parameterizing the soft-prompt. The two-layer MLP includes two linear layers with the ReLU activation function. The number of hidden nodes in the hidden layer is set to 512 in all Q-tuning experiments.

D More Ablation Study Results

Table 11 reports more details of the results on each order in Table 5 for the ablation study. Table 12 presents the effectiveness of setting different memory factors η in the MR loss. As shown, the η is suggested to 10^{-2} for the long sequence tasks. By

comparing with the results of “w/o MR”, the performance by using MR loss is improved by 1.7% on average.

Table 12: Ablation study experiments (20 samples/class for long sequence) on the memory factor η of the MR loss. All results are averaged over 3 runs.

Parameter	Long Sequence			
	Order 8	Order 9	Order 10	Average
$\eta = 1$	73.5	75.8	73.2	74.2
$\eta = 10^{-1}$	77.1	78.6	77.3	77.7
$\eta = 10^{-2}$	78.3	79.7	78.7	78.9
$\eta = 10^{-3}$	78.1	79.4	78.0	78.5
$\eta = 10^{-4}$	77.8	78.8	77.8	78.1
w/o MR	77.3	77.3	77.1	77.2

E Evaluation of Forward Transfer and Backward Transfer

We compare the forward transfer and backward transfer performance of Q-tuning with the competitors using the metrics defined by (Lopez-Paz and Ranzato, 2017) in the long-sequence experiments. Table 13a and Table 13b report the forward knowledge transfer performance and backward knowledge transfer performance across 3 task orders (Or-

der 8, Order 9, Order 10) of long-sequence experiments. Figures 3, 4 and 5 show the forward transfer scores of the order 8 task sequence. Figures 6, 7 and 8 show the forward transfer scores of the order 9 task sequence, and Figures 9, 10 and 11 show the forward transfer scores of the order 10 task sequence.

Method	Few-shot (20 samples/class)	Full-shot
Finetune	16.9	16.0
Data Replay	16.8	14.0
Prompt Tuning	23.1	24.9
Per-task Prompt	0	0
LFPT5	18.9	24.9
ProgPrompt*	21.1	24.7
Q-tuning (Ours)	26.7	29.7

(a) The average forward knowledge transfer performance across 3 task orders (Order 8, Order 9, Order 10) of long-sequence experiments.

Method	Few-shot (20 samples/class)	Full-shot
Finetune	-59.5	-63.5
Data Replay	-24.7	-18.0
Prompt Tuning	-47.9	-71.0
Per-task Prompt	0	0
LFPT5	-13.5	-8.8
ProgPrompt*	0	0
Q-tuning (Ours)	0	0

(b) The average backward knowledge transfer performance across 3 task orders (Order 8, Order 9, Order 10) of long-sequence experiments.

Table 13: Average performance of the forward and backward knowledge transfer with the T5 model on the long-sequence benchmark.

Figures 12, 13 and 14 show the backward transfer scores of the order 8 task sequence, Figures 15, 16 and 17 show the backward transfer scores of the order 9 task sequence, and Figures 18, 19 and 20 show the backward transfer scores of the order 10 task sequence. In these backward transfer measurements, the score 0 stands for not forgetting old tasks. The evolution of the average accuracy over learning new tasks (Lopez-Paz and Ranzato, 2017) are reported in Figure 21.

Order 8 (20 samples/class)

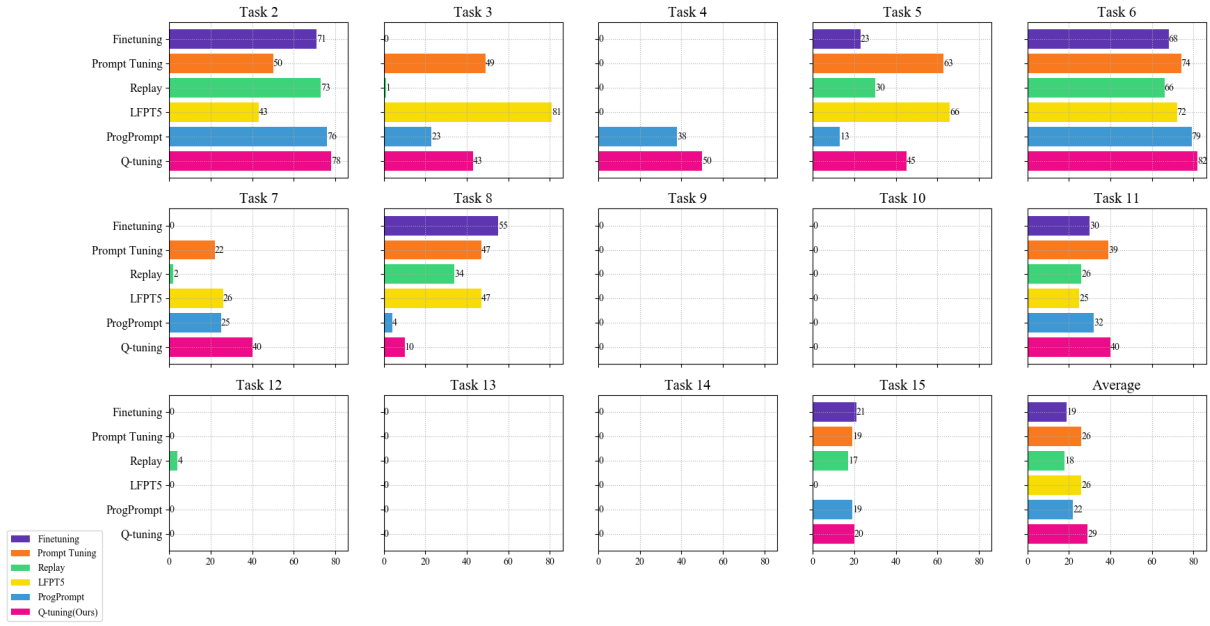


Figure 3: Forward transfer score of different approaches on the order 8 (20 samples/class).

Order 8 (200 samples/class)

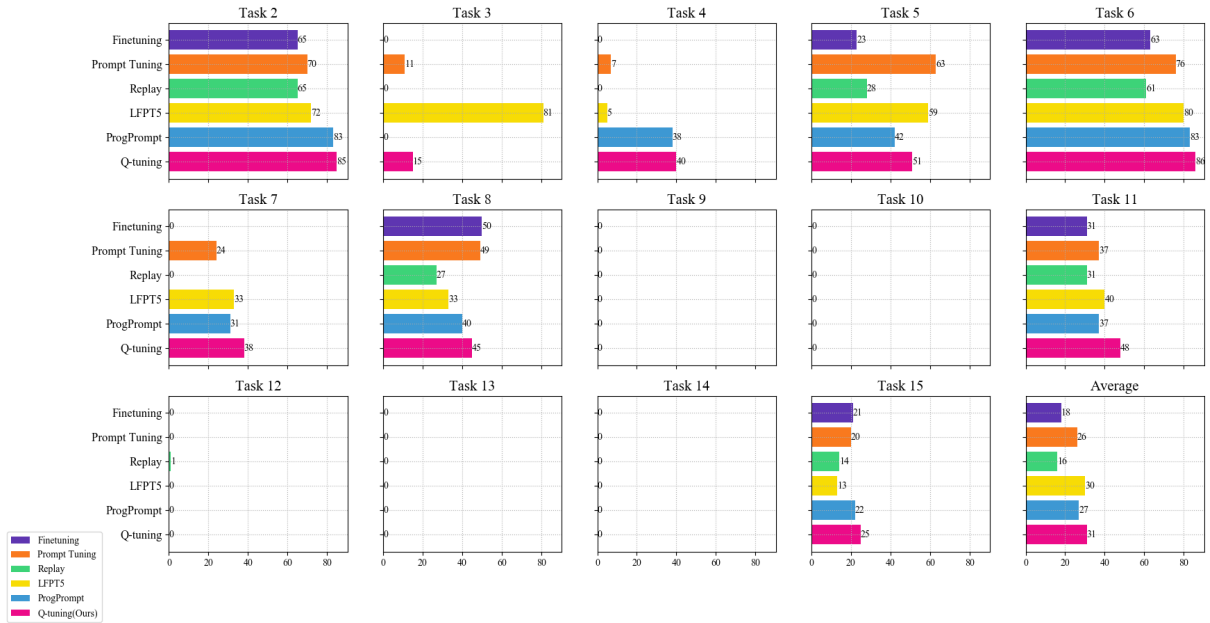


Figure 4: Forward transfer score of different approaches on the order 8 (200 samples/class).

Order 8 (1000 samples/class)

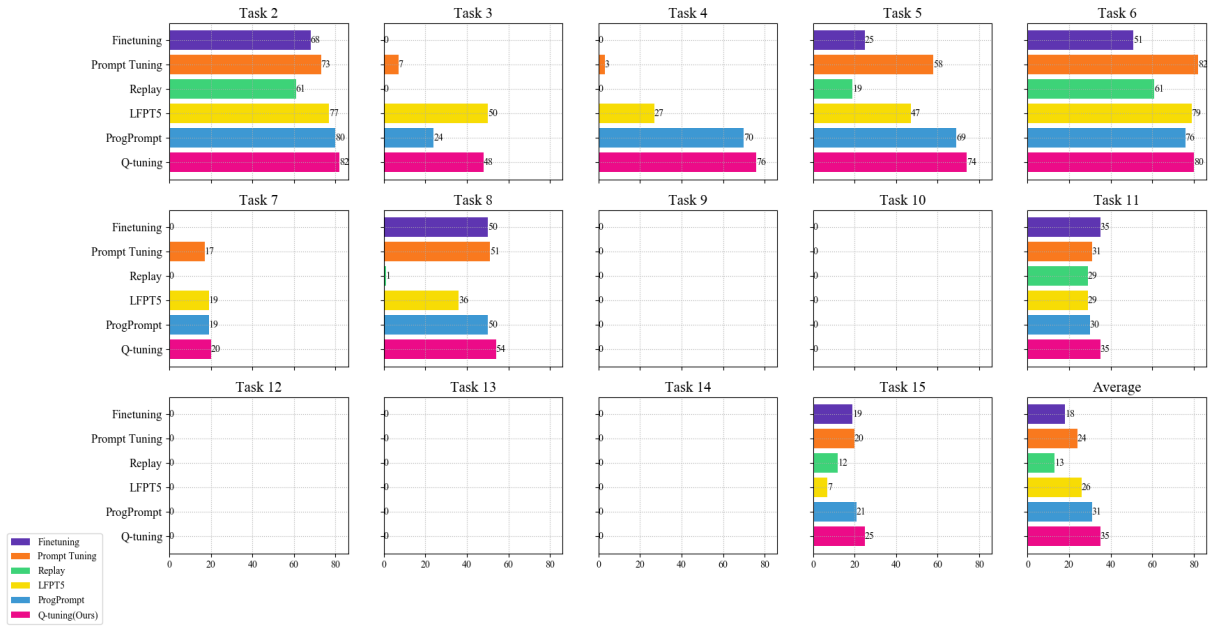


Figure 5: Forward transfer score of different approaches on the order 8 (1000 samples/class).

Order 9 (20 samples/class)

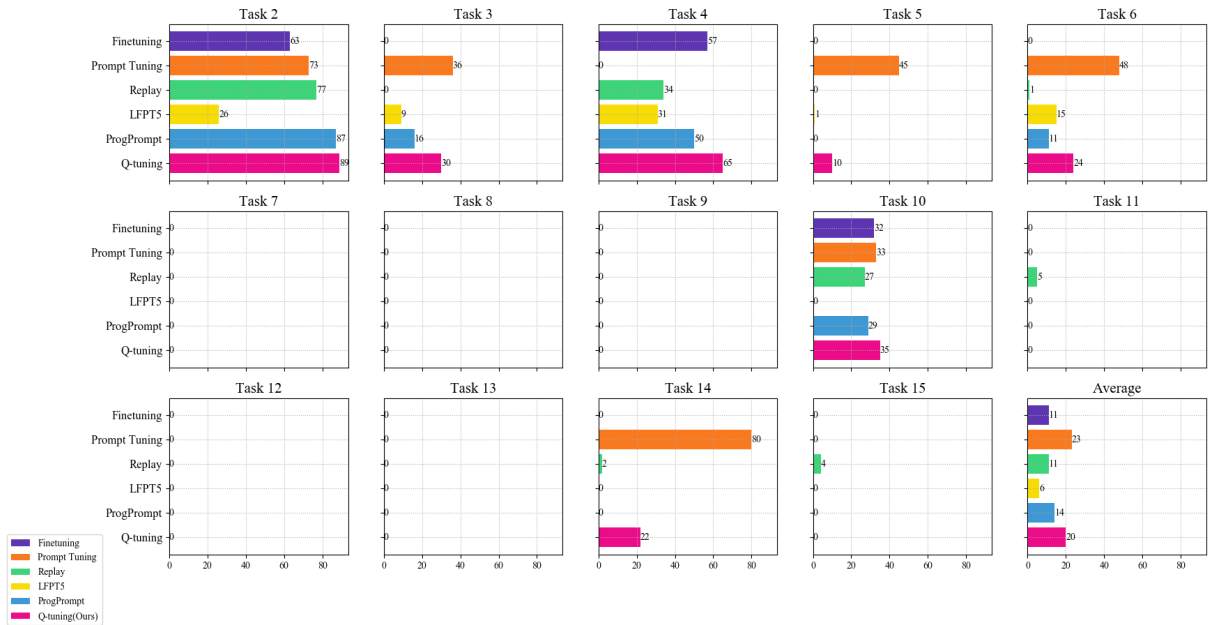


Figure 6: Forward transfer score of different approaches on the order 9 (20 samples/class).

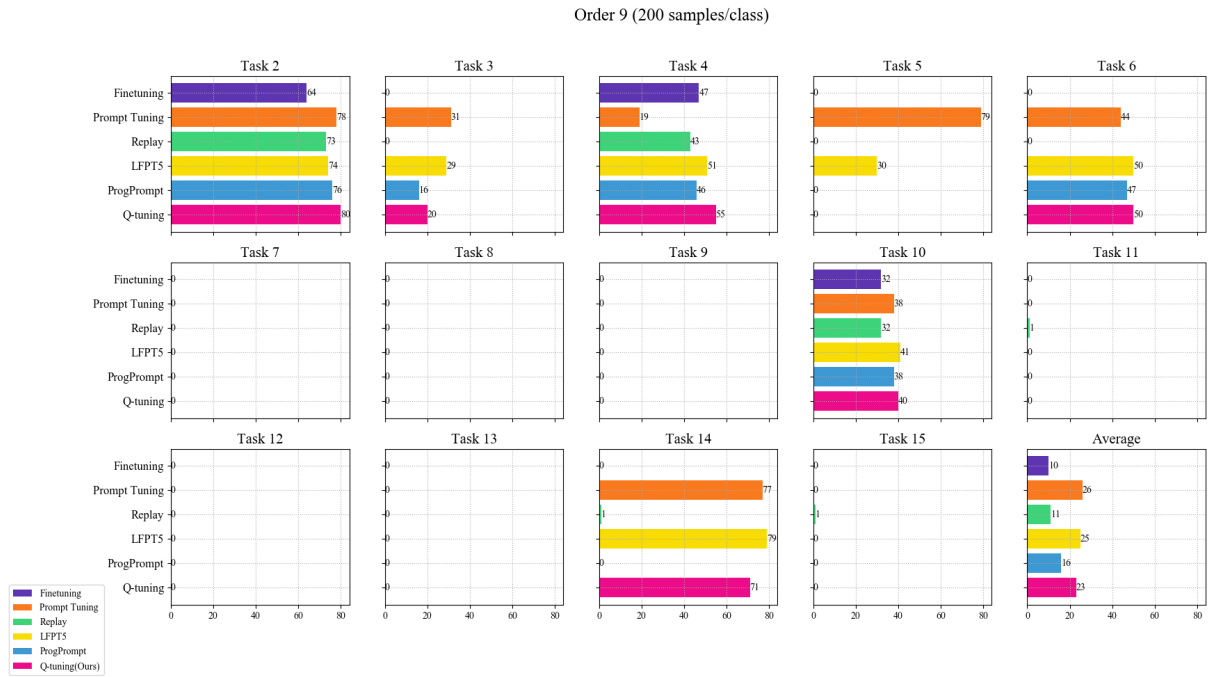


Figure 7: Forward transfer score of different approaches on the order 9 (200 samples/class).

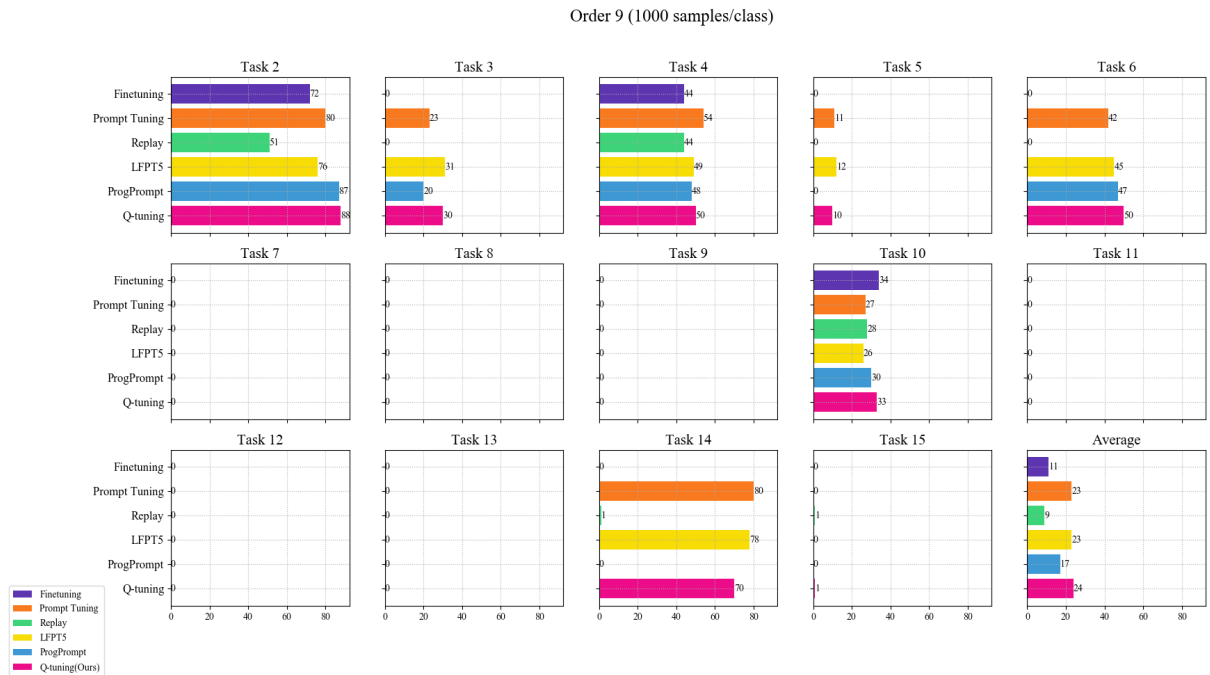


Figure 8: Forward transfer score of different approaches on the order 9 (1000 samples/class).

Order 10 (20 samples/class)

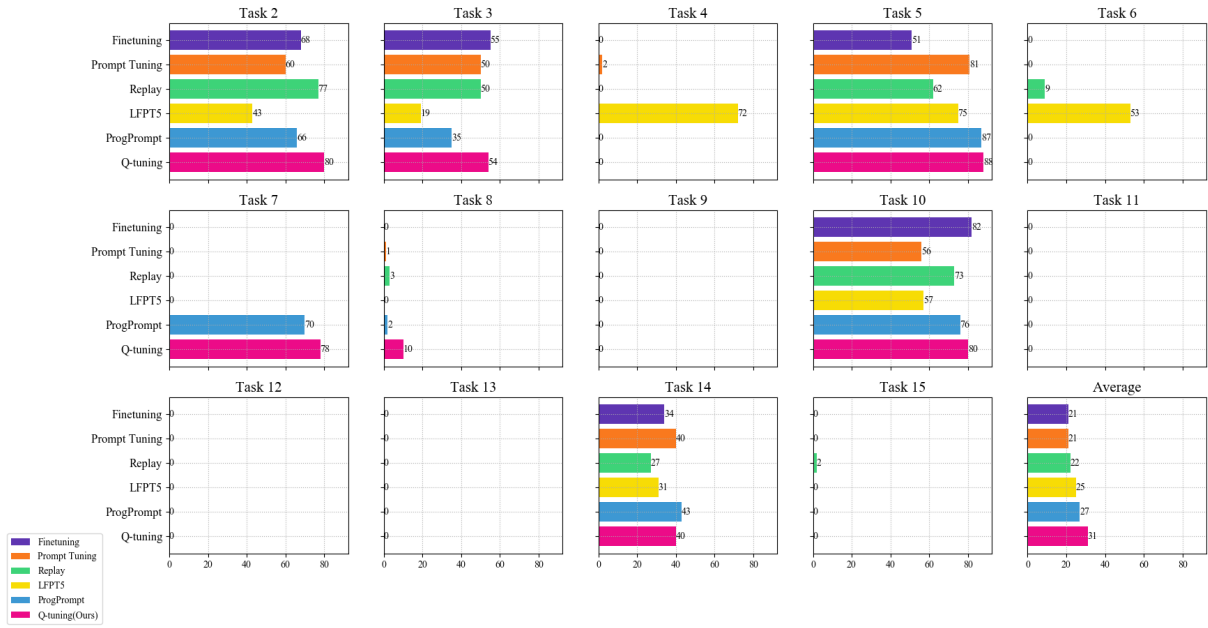


Figure 9: Forward transfer score of different approaches on the order 10 (20 samples/class).

Order 10 (200 samples/class)

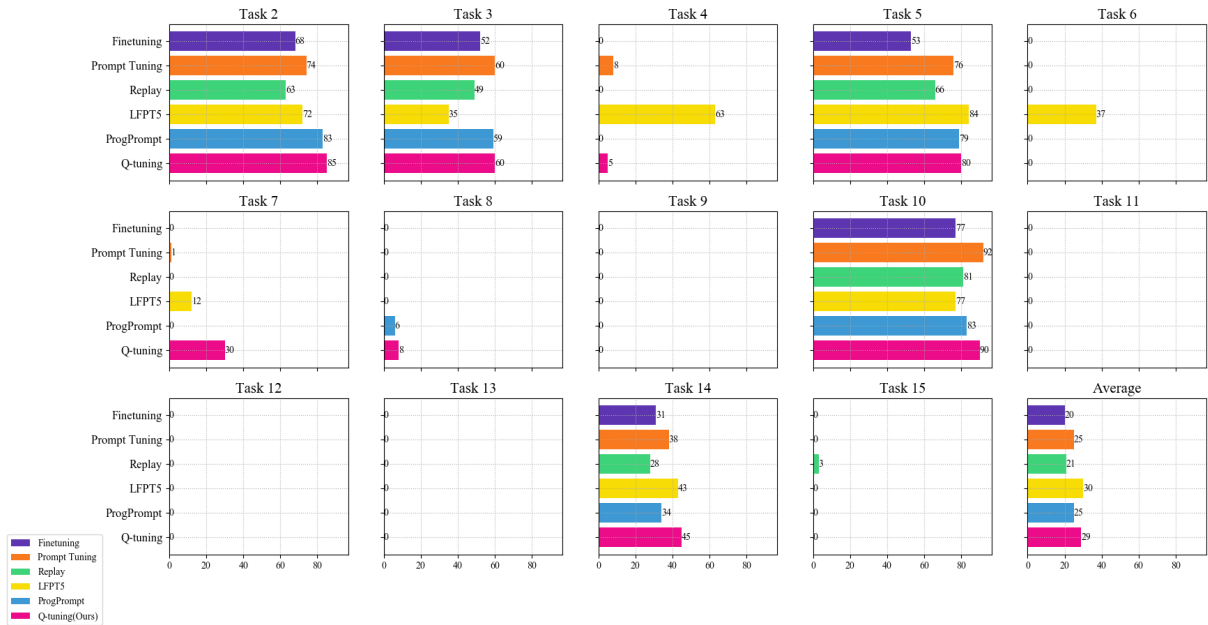


Figure 10: Forward transfer score of different approaches on the order 10 (200 samples/class).

Order 10 (1000 samples/class)

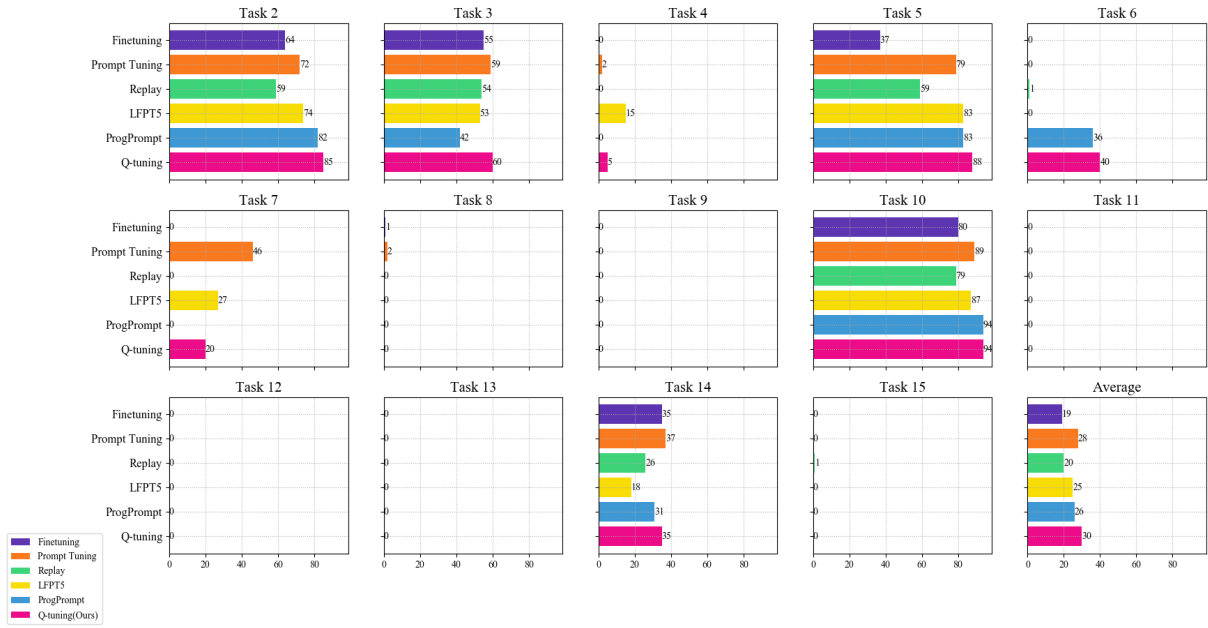


Figure 11: Forward transfer score of different approaches on the order 10 (1000 samples/class).

Order 8 (20 samples/class)

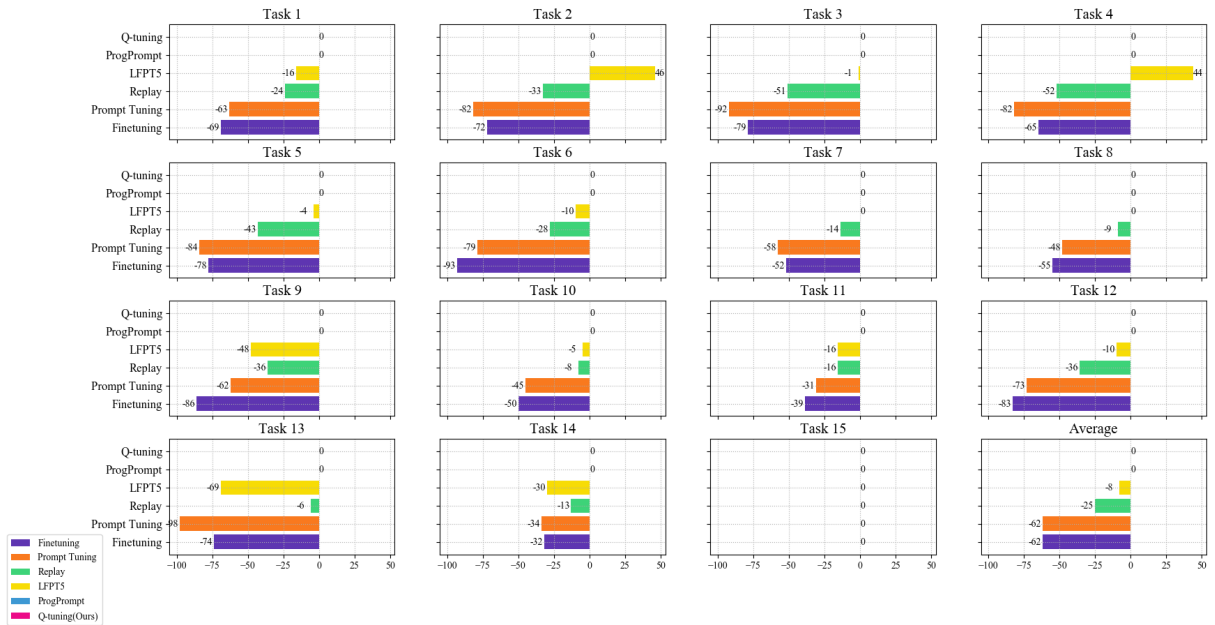


Figure 12: Backward transfer score of different approaches on the order 8 (20 samples/class).

Order 8 (200 samples/class)

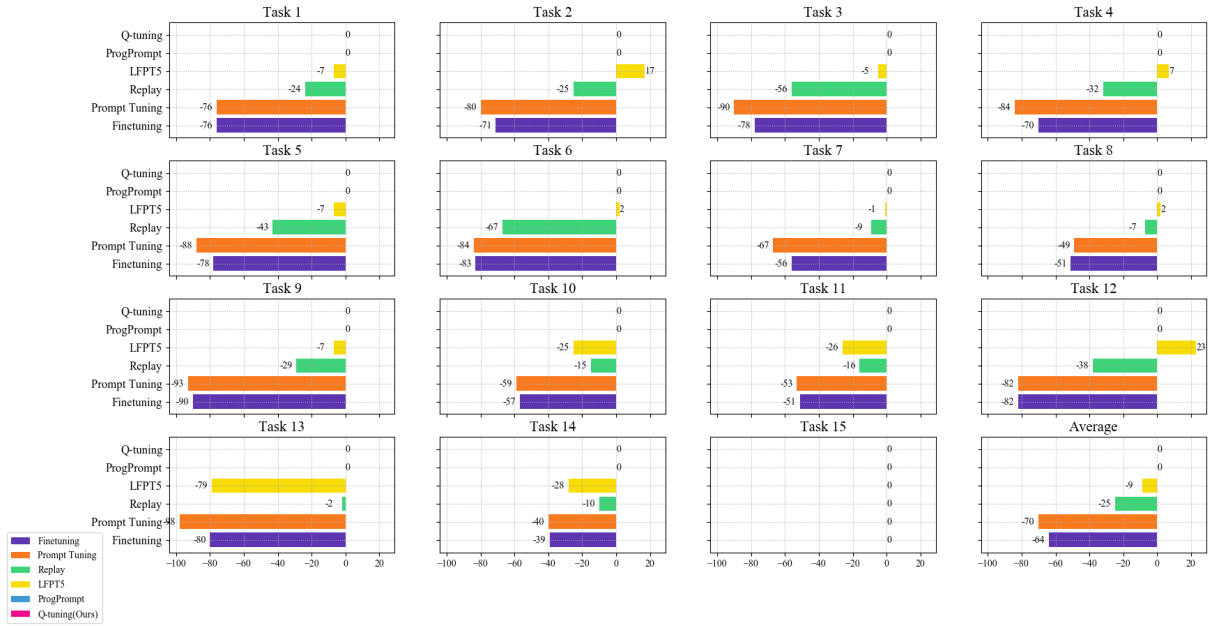


Figure 13: Backward transfer score of different approaches on the order 8 (200 samples/class).

Order 8 (1000 samples/class)

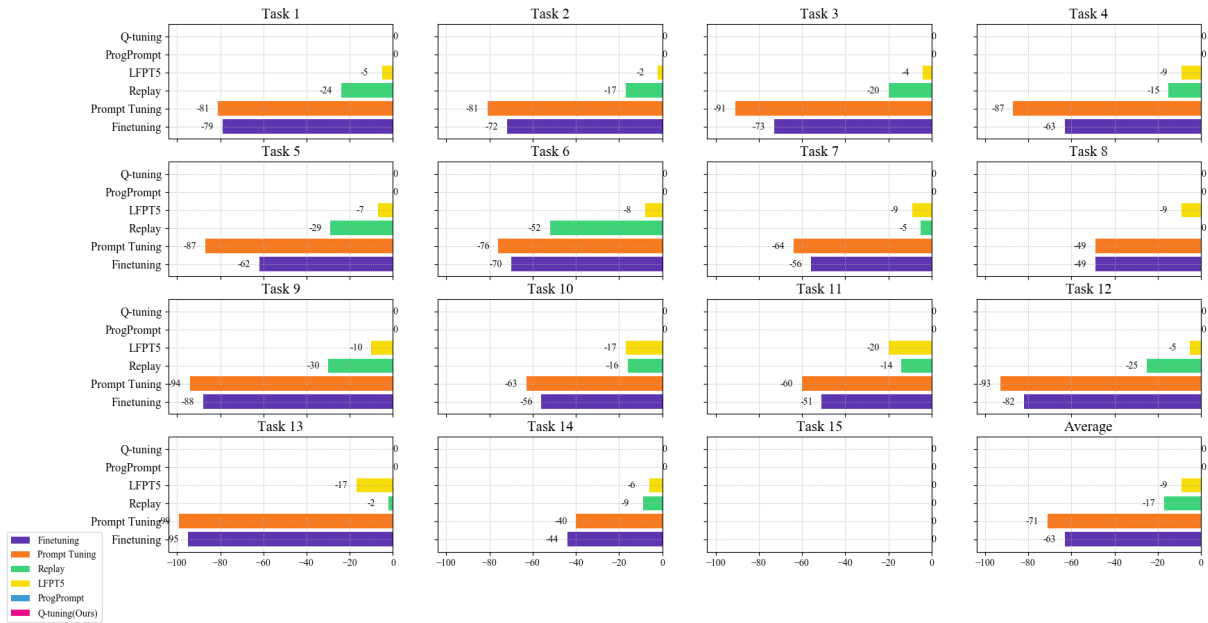


Figure 14: Backward transfer score of different approaches on the order 8 (1000 samples/class).

Order 9 (20 samples/class)

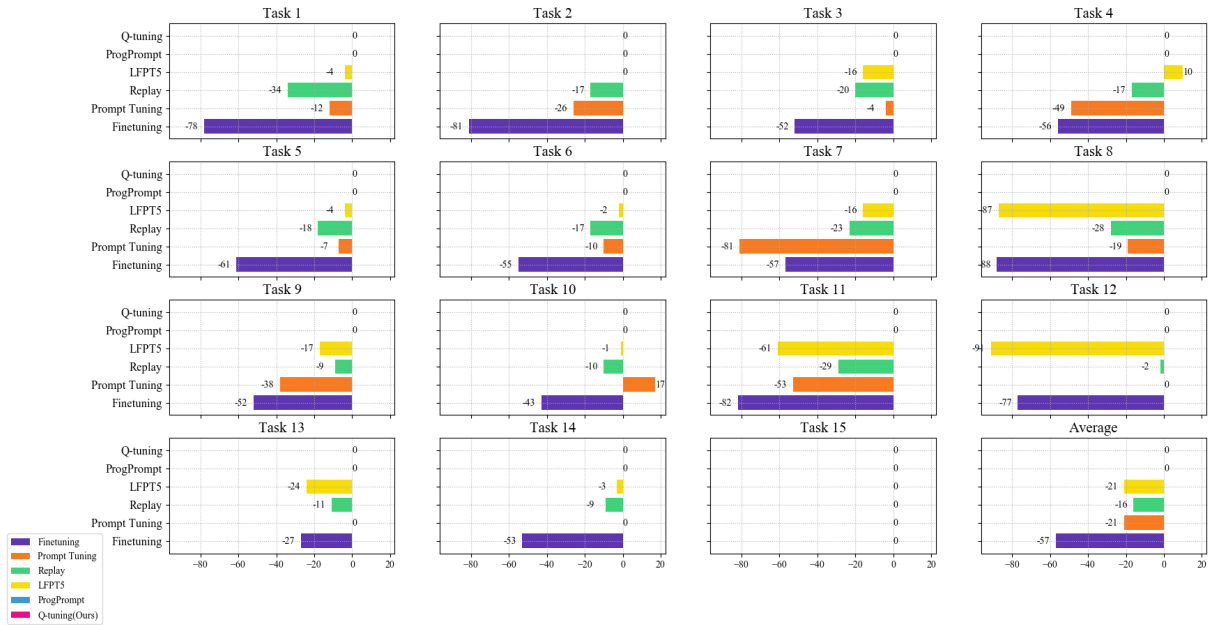


Figure 15: Backward transfer score of different approaches on the order 9 (20 samples/class).

Order 9 (200 samples/class)

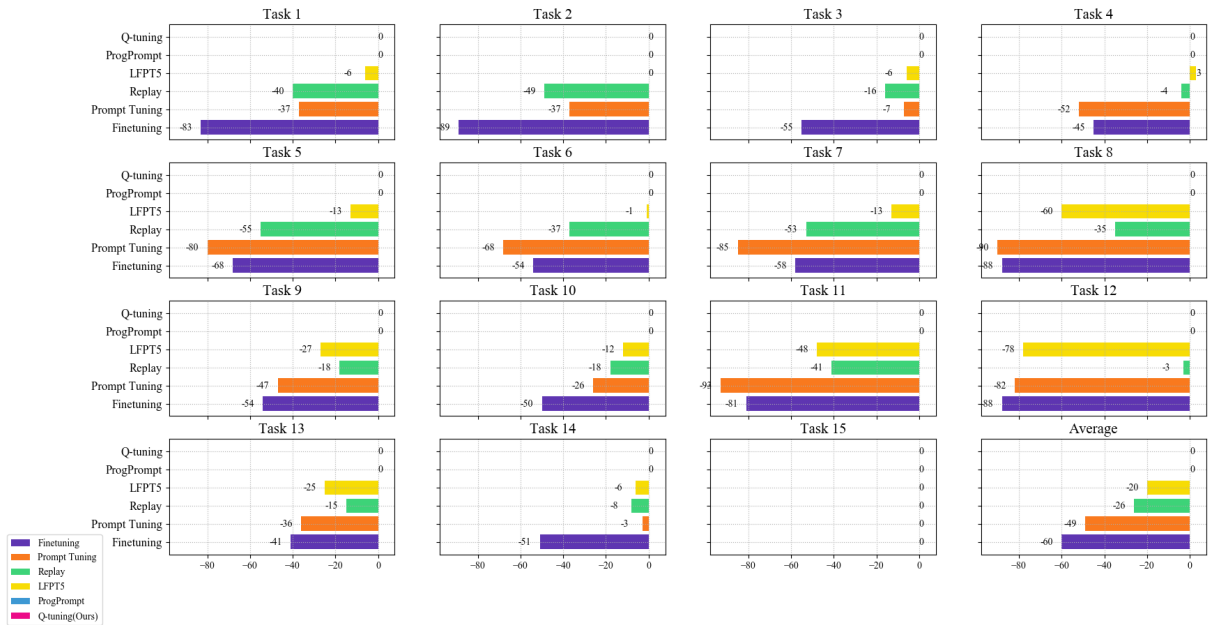


Figure 16: Backward transfer score of different approaches on the order 9 (200 samples/class).

Order 9 (1000 samples/class)

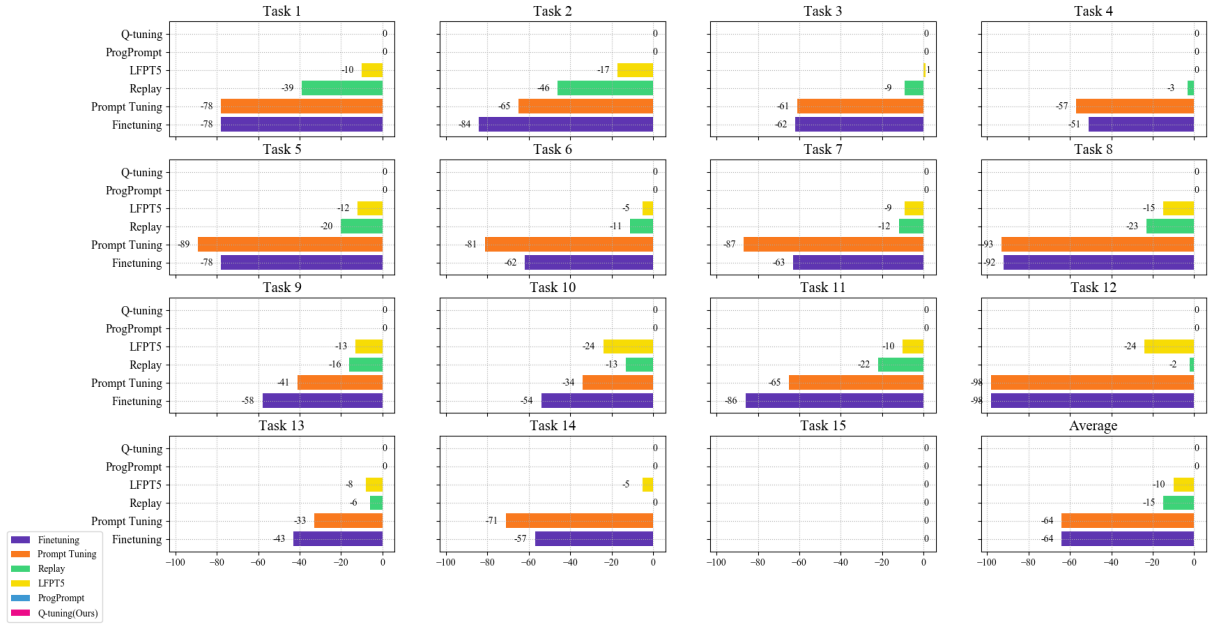


Figure 17: Backward transfer score of different approaches on the order 9 (1000 samples/class).

Order 10 (20 samples/class)

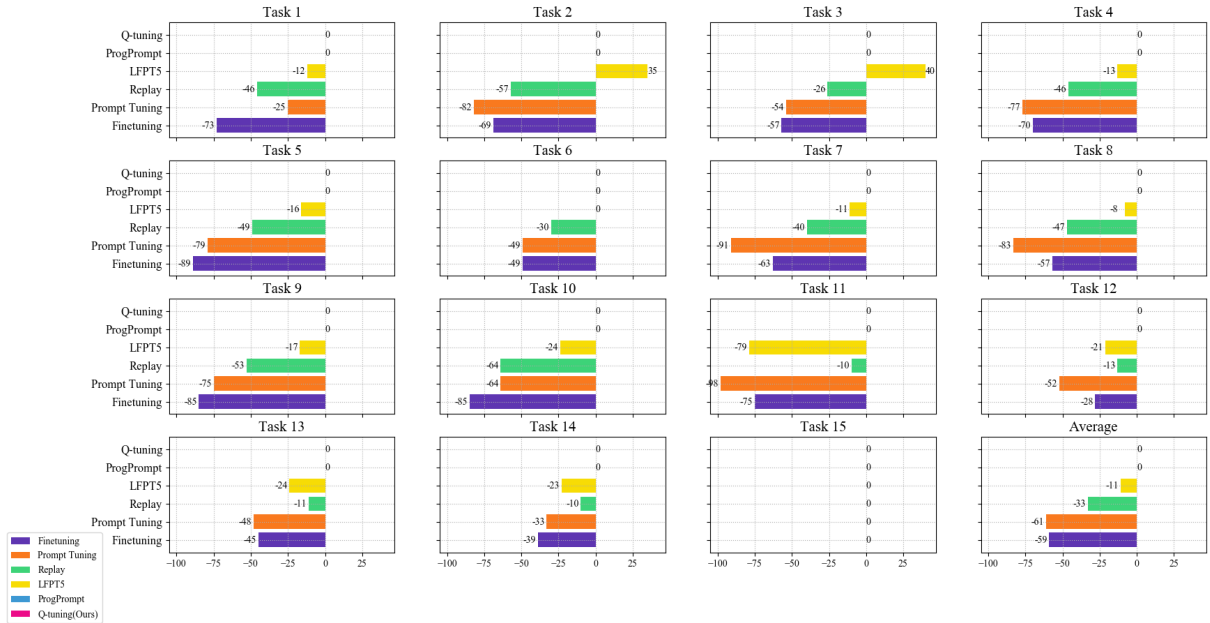


Figure 18: Backward transfer score of different approaches on the order 10 (20 samples/class).

Order 10 (200 samples/class)

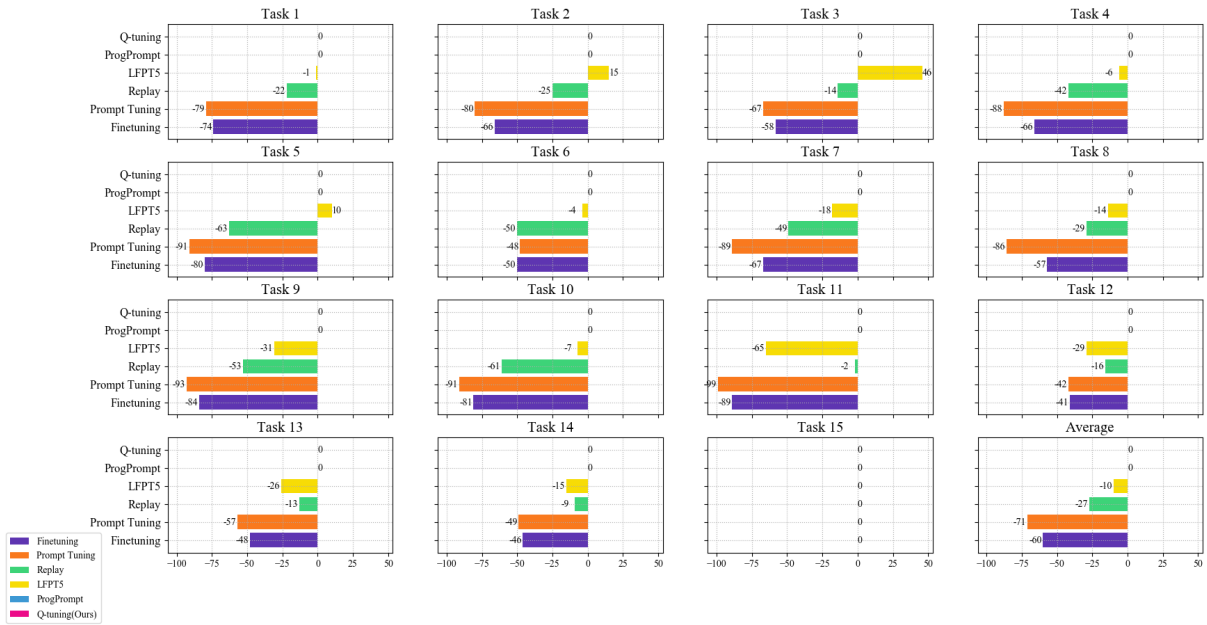


Figure 19: Backward transfer score of different approaches on the order 10 (200 samples/class).

Order 10 (1000 samples/class)

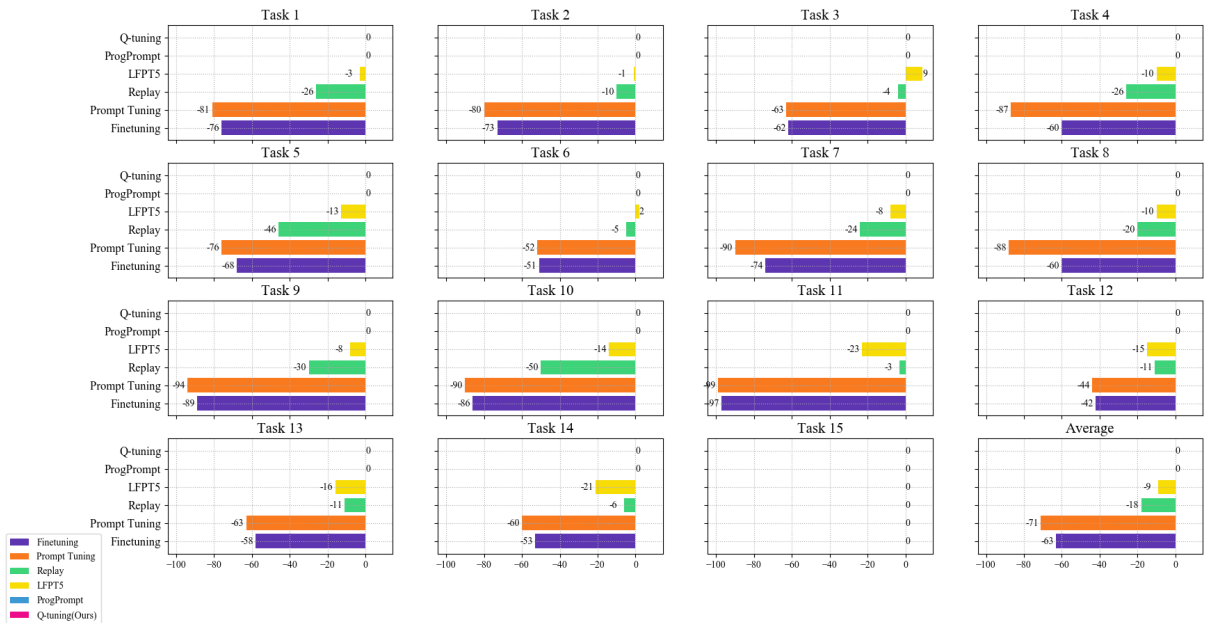


Figure 20: Backward transfer score of different approaches on the order 10 (1000 samples/class).

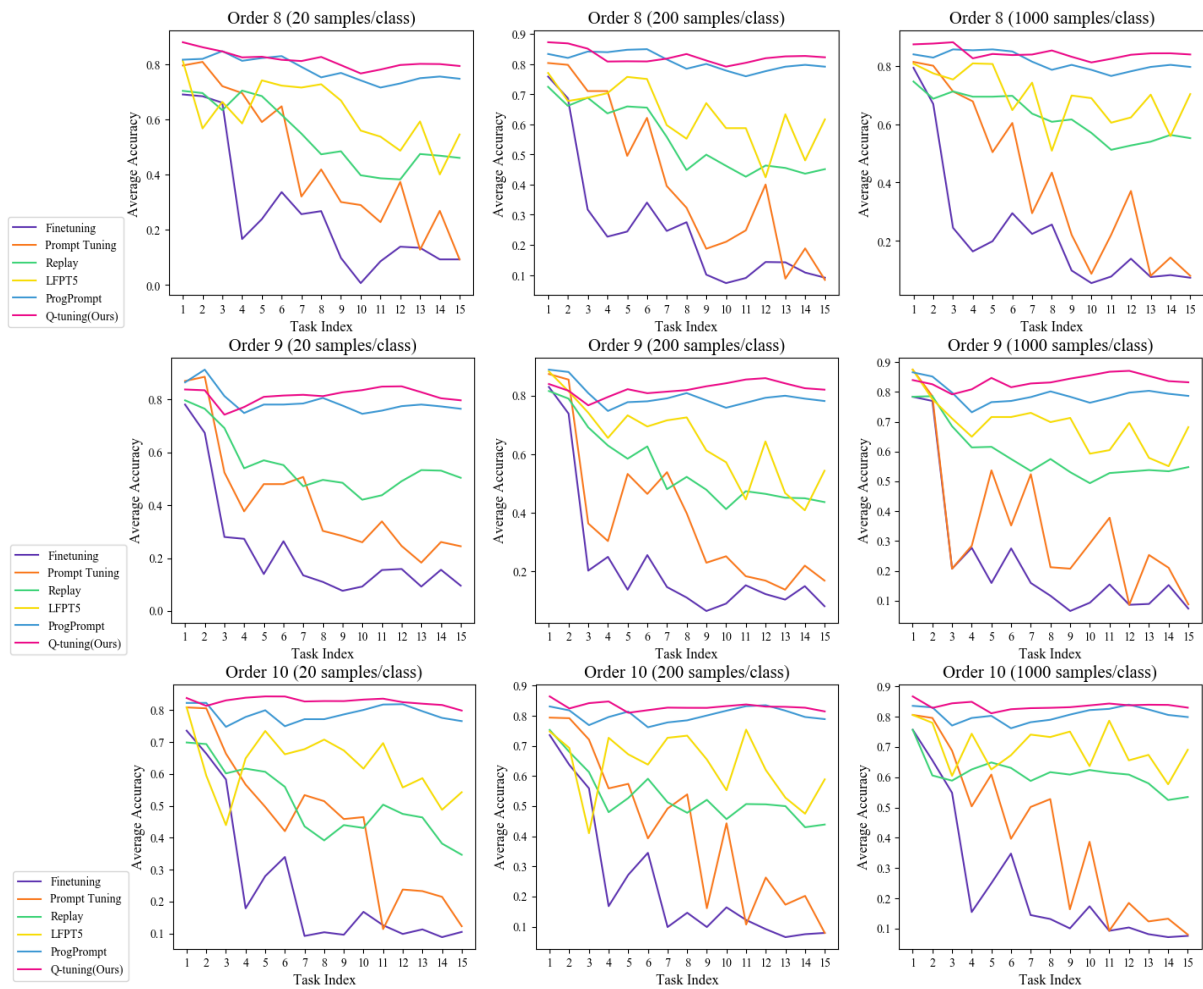


Figure 21: Evolution of average accuracy after learning new tasks.